Chaos
An Interdisciplinary Journal of Nonlinear Science

RESEARCH ARTICLE | JANUARY 15 2025

Modeling shock propagation and resilience in financial temporal networks

Fabrizio Lillo ; Giorgio Rizzini

Chaos 35, 013134 (2025)
https://doi.org/10.1063/5.0244665

Modeling shock propagation and resilience in financial temporal networks

Cite as: Chaos 35, 013134 (2025); doi: 10.1063/5.0244665
Submitted: 21 October 2024 · Accepted: 24 December 2024 ·
Published Online: 15 January 2025

Fabrizio Lillo[1,2,a] and Giorgio Rizzini[2,b]

AFFILIATIONS

[1]Dipartimento di Matematica, Università degli Studi di Bologna, Piazza di Porta San Donato 5, 40126 Bologna, Italy
[2]Classe di Scienze, Scuola Normale Superiore, Piazza dei Cavalieri 7, 56126 Pisa, Italy

[a]**Electronic mail:** fabrizio.lillo@sns.it
[b]**Author to whom correspondence should be addressed:** giorgio.rizzini@sns.it

ABSTRACT

Modeling how a shock propagates in a temporal network and how the system relaxes back to equilibrium is challenging but important in many applications, such as financial systemic risk. Most studies, so far, have focused on shocks hitting a link of the network, while often it is the node and its propensity to be connected that are affected by a shock. Using the configuration model—a specific exponential random graph model—as a starting point, we propose a vector autoregressive (VAR) framework to analytically compute the Impulse Response Function (IRF) of a network metric conditional to a shock on a node. Unlike the standard VAR, the model is a nonlinear function of the shock size and the IRF depends on the state of the network at the shock time. We propose a novel econometric estimation method that combines the maximum likelihood estimation and Kalman filter to estimate the dynamics of the latent parameters and compute the IRF, and we apply the proposed methodology to the dynamical network describing the electronic market of interbank deposit.

This paper proposes a new mathematical model to quantify how a shock modifies the structure of a temporal network, as well as establish how the system relaxes back to the pre-shock condition. The novel methodology incorporates dynamic latent variables that characterize nodes' propensity to create links. Since the latent variables are not observable, this paper also proposes an estimation method to capture the latent variables' dynamics based on the Kalman filter approach. An empirical application to the interbank market shows that the proposed approach provides meaningful insights into the propagation of systemic risk, following a shock hitting one of the banks.

I. INTRODUCTION

Understanding how a shock spreads across a system and how it relaxes back to equilibrium is important, yet hard, and it remains an open task in many complex systems. Recently, the theory of complex networks has been widely adopted in many different fields (see, for example, Boccaletti *et al.*, 2006; Estrada, 2012; and Mata, 2020) to model the interconnections between different parts of the system. Moreover, an additional challenge is brought about by the dynamical nature of the interactions, leading to the representation of the system in terms of temporal networks. In fact, a shock modifies not only the instantaneous structure of the network but also, more importantly, its dynamics and the appearance of links in future times, since the network reorganizes itself in response to the shock. This makes the problem particularly challenging and requiring a careful modeling as recently reviewed in Artime *et al.* (2024).

The purpose of this paper is to provide a general modeling framework for studying the propagation of a shock in a temporal network. Unlike other approaches (see, for example, Giraitis *et al.*, 2016), we are interested in studying the evolution of the system when a node (or a subset of nodes) is shocked (see, among others, Eisenberg and Noe, 2001; Glasserman and Young, 2015; Glasserman and Young, 2016; Cerqueti *et al.*, 2023; and the review of Bardoscia *et al.*, 2021 in a financial context), rather than considering the case when a link is shocked (for example, it disappears). Since, different from links, both nodes' properties and their propensity to create connections are not always visible, we propose to use a model with node-specific quantities. More specifically, we resort

to the celebrated configuration or fitness model (see Holland and Leinhardt, 1981; Bianconi and Barabási, 2001; Caldarelli *et al.*, 2002; Chatterjee *et al.*, 2011; and Yan *et al.*, 2018), a specific instance of the exponential random graph family (Lusher *et al.*, 2013 and Harris, 2013), which associates to each node (one or two in the directed network case) latent variable, termed fitness, describing the propensity of the node to create links. A link between two nodes is created with a probability depending on the fitness of the two nodes. Since the original model describes static networks, here, we extend it by assuming that the fitness evolves according to a vector autoregressive model of order one, VAR(1). Recently, Mazzarisi *et al.* (2020) introduced a dynamical version of the fitness model, assuming an independent dynamics of each latent variable. On the contrary, our VAR approach allows us to model the lagged correlations between latent variables, i.e., how the propensity of a node in creating a link at time t is correlated with the propensity of another node in creating a link at a future time. This is fundamental for modeling shock propagation since it allows us to flexibly describe these lagged interactions between nodes.

Leveraging on the vast literature on VAR models (Lütkepohl, 2010), we propose a modification of the Impulse Response Function (IRF) for temporal networks. We remind that, loosely speaking, the IRF describes the expected dynamics of a variable conditional to a shock at initial time. However, different from the standard VAR model, we are interested in studying the IRF for a *network metric*, a function of the adjacency matrix describing the graph, e.g., its density, clustering coefficient, diameter, etc. To the best of our knowledge, our paper is the first to propose IRF analysis on a network metric. In particular, the aim is to analyze the variation of a given network metric in a dynamic setting after which a node's fitness has been shocked. Additionally, we analyze how the system relaxes back to the equilibrium state by also examining the recovery time.

Since the VAR model describes the fitnesses' dynamics, the IRF of a network metric has very different properties with respect to linear models. First, we show that it is a nonlinear function of the shock size, i.e., doubling the shock size does not lead to doubling the effect. Second, the conditional dynamics of the network metric depends on the initial state of the network, while in the standard VAR model, it is independent from the initial and past states of the system. Thus, in a networked system, the timing of the shock has important consequences on the shock's propagation and relaxation dynamics.

As mentioned, our approach allows us to construct IRF scenarios by considering the shocks on nodes. As we detail in Sec. III, latent variables often correlate with node-specific quantities and are more directly affected by shocks. For example, in interbank networks, fitnesses strongly correlate with bank exposure, and in the World Trade Web, they correlate with the Gross Domestic Product (GDP). Thus, a shock on fitness corresponds to a shock on these variables, which clearly describes the propensity of the nodes (banks, country) to create links. Second, in a network with n nodes, the number of latent variables is $O(n)$, while the number of links is $O(n^2)$. Thus, a model based on node variables is much more parsimonious than one based on links and presents a much smaller risk of overfitting. Finally, our methodology is flexible enough to describe the situation in which a node, at a certain time, could delete all its links (as if the node were removed) and, at future times, has the chance to connect with other nodes in the network.

Despite the fact that the proposed approach in this paper is general, our main application will be on financial networks. Networks have been widely applied to economics and financial systems where many market participants (e.g., investors, banks, firms) interact with each other with possibly different types of interactions. In this field, the interest for shock propagation and system's resilience is intimately related to the assessment of systemic risk. Since the United States subprime crisis, the European sovereign debt crisis in 2008, and the COVID-19 crisis, it became clear how fragile and interconnected the economic and financial systems are; see, among others, Ackermann (2008), Sanders (2008), Allen and Carletti (2010), Easley *et al.* (2010), and Caccioli *et al.* (2018) for a review on financial networks and systemic risk. The enormous consequences of a financial shock are crucial to analyzing how a system reacts in order to minimize economic, financial, and social damages. An important aspect is unveiling not only the path with which an external shock propagates within the system but also quantifying the resilience of the system in terms of shock absorption and recovery time (see, for example, May *et al.*, 2008; Holme and Saramäki, 2012; and Battiston *et al.*, 2016). Resilience in complex networks has been studied, for example, in Albert *et al.* (2000), Gao *et al.* (2016), Ferraro and Iovanella (2018), and Artime *et al.* (2024); although most of the studies have been focused on the resilience of static networks, our focus is on temporal networks.

In the last part of this paper, we propose a method to estimate the latent VAR parameters from empirical data. This is needed to construct IRFs for the real problem at hand. We propose a novel estimation method of the model by an approach combining the maximum likelihood estimation (MLE) method and the Kalman filter. Interestingly, a different use of the Kalman filter procedure for modeling the estimation of exponential random graph parameters was recently proposed by Buccheri and Mazzarisi (2024). We test the accuracy of our procedure on synthetic networks, confirming the improvement in the accuracy of our methodology in the estimation of latent variables and static parameters. As an empirical illustration, we estimate the model and compute the IRF on a dataset describing the evolution of the financial directed network of the electronic Market of Interbank Deposit (e-MID), whose topological properties and financial implications have been intensively studied in previous works (Iori *et al.*, 2006; Iori *et al.*, 2008; Iori *et al.*, 2015; Fricke and Lux, 2015a; 2015b; Barucca and Lillo, 2016; Temizsoy *et al.*, 2017; and Barucca and Lillo, 2018) for its role in systemic risk.

This paper is structured as follows. Section II introduces the main background and preliminary concepts of temporal networks and the fitness model, as well as the analytical formulation of the expected value of a network metric in a stochastic environment. Section III presents the general formulation of the impulse response function for a temporal network. Section IV analyzes the IRF in a specific solvable framework as well as the role of each model's parameter in shock spreading. Section V introduces the novel econometric procedure based on the Kalman filter to estimate the fitnesses' dynamics, the results of numerical simulations, and the application of the model to the e-MID interbank network. Conclusions follow.

II. NETWORKS AND FITNESS MODEL

The derivation of the impulse response function in Sec. III applies to both directed and undirected unweighted networks, but we consider them differently in the following. Specifically, in Sec. IV, we derive a closed-form solution for the IRF in the case of undirected graphs in a specific analytically solvable case, while in Sec. V, we estimate the model and simulate the impulse response function for the (directed) e-MID network. For these reasons, this section outlines the main concepts of both undirected and directed networks, along with their associated fitness models that will be used in the temporal network setting.

Preliminary concepts on networks. A network is represented by a graph $G = (V, E)$, where V is the set of n nodes and E is the set of links connecting the nodes. Let $|E|$ be the number of links. We say that two nodes $i, j \in V$ are connected if there is a link between them, i.e., if $(i, j) \in E$. We assume that the network is unweighted, that is, if a link exists, then its weight is one. A graph is said undirected if $(i, j) \in E$ implies that $(j, i) \in E$. The topology of the network can be represented by a symmetric $n \times n$ matrix adjacency matrix $\mathbf{A}$. The entries of $\mathbf{A}$ are $a_{ij} = 1$ if $(i, j) \in E$, zero otherwise. No self-loops are allowed, that is, $a_{ii} = 0$ for $i = 1, \ldots, n$. A network is directed if $(i, j) \in E$ does not imply that $(j, i) \in E$ and the topology is described by a non-symmetric adjacency matrix $\mathbf{A}$. A scalar function on a network $f : \{0, 1\}^{n\times n} \to \mathbb{R}$ maps elements from the space of the adjacency matrices of order n to real numbers, such as density, assortativity coefficient, and average clustering coefficient. Network density measures the proportion of existing links between nodes with respect to the possible ones and is defined as

$$\delta = \frac{\sum_{i,j} a_{ij}}{n(n-1)}. \tag{1}$$

In the case of an undirected network, Eq. (1) gives $\delta = \frac{2|E|}{n(n-1)}$, whereas for a directed network, it is $\delta = \frac{|E|}{n(n-1)}$. For a node i, its degree expresses the number of links incident on it, i.e., $d_i = \mathbf{A}\vec{\mathbf{1}}$, where $\vec{\mathbf{1}}$ is a vector of ones of dimension n. In directed graphs, the direction of the arc matters and, therefore, the degree of a node can be split into in-degree and out-degree. For any vertex i, the in-degree is the number of incoming links while the out-degree is the number of outgoing links. The in- and out-degrees can be represented in terms of the adjacency matrix as follows:

$$d_i^{in} = \mathbf{A}_i^T\vec{\mathbf{1}}, \quad d_i^{out} = \mathbf{A}_i\vec{\mathbf{1}},$$

where $\mathbf{A}_i$ corresponds to the ith row of matrix $\mathbf{A}$ and $\mathbf{A}^T$ is the transpose of matrix $\mathbf{A}$.

Fitness model for static networks. A fitness (or configuration) model is a latent variable approach to networks. It has been introduced, more or less independently, many times in the last decades; see, among others, Holland and Leinhardt (1981), Bianconi and Barabási (2001), Caldarelli *et al.* (2002), Chatterjee *et al.* (2011), and Yan *et al.* (2018). In a static undirected network, each node i is associated with a latent parameter, θ_i, termed *fitness*, describing the propensity of the node to create links, whereas, in a directed network, each node i is associated with two latent parameters, θ_i^{in} and θ_i^{out}, describing the propensity of the node to create incoming and outgoing links, respectively. Then, for each pair of nodes i and j, a link between them is created with probability $g(\theta_i, \theta_j)$, where g is the *link function*. In the directed case, an arc from node i to node j is created with probability $g(\theta_i^{out}, \theta_j^{in})$. It is important to stress that arcs are generated independently (even if, obviously, they are not identically distributed). Different functional forms for g can be used. In this paper, we use the (standard) logistic form

$$g(\theta_i, \theta_j) := P(a_{ij} = 1|\theta_i, \theta_j) = \frac{1}{1 + e^{-\theta_i-\theta_j}}, \quad \forall i, j \in V \tag{2}$$

for undirected networks and

$$g(\theta_i^{out}, \theta_j^{in}) := P(a_{ij} = 1|\theta_i^{out}, \theta_j^{in}) = \frac{1}{1 + e^{-\theta_i^{out}-\theta_j^{in}}}, \quad \forall i, j \in V \tag{3}$$

for directed networks. With this choice of the link function, the domain of θs is the whole real axis. Notice that, when all θs are the same, the ensemble of networks is one of the celebrated Erdös–Renyi random graph model. From Eqs. (2) and (3), it is clear that the degree of a node depends strongly on its fitness. We underline that this paper focuses only on unweighted networks, while a possible extension to weighted graphs could be done by following the approach in Gabrielli *et al.* (2019).

The choice of the logistic function for g is made because it connects the fitness model with the class of exponential random graphs models (see Lusher *et al.*, 2013 and Harris, 2013). Exponential random graphs are probability distributions of graphs belonging to the exponential family, that is,

$$P(\mathbf{A}|\vec{\boldsymbol{\theta}}) = \frac{\exp\left(\sum_{i=1}^{q} \theta_i f_i(\mathbf{A})\right)}{Z(\vec{\boldsymbol{\theta}})}. \tag{4}$$

$\vec{\boldsymbol{\theta}} \in \mathbb{R}^q$ is a vector collecting the latent variables that influence the topology, f_i is a network metric that is also a sufficient statistic for the distribution, and $Z(\vec{\boldsymbol{\theta}})$ is a normalization factor ensuring that $P(\mathbf{A}|\vec{\boldsymbol{\theta}})$ is a well-defined probability mass function. Choosing the total number of links (or equivalently, the density) as a unique sufficient statistic and assuming undirected and unweighted networks, so that $q = 1$, Eq. (4) reduces to the Erdös–Renyi model (see Erdos and Renyi, 1959). When in an undirected network all degrees of the nodes are considered as sufficient statistics, i.e., $q = n$ and $f_i = d_i$, Eq. (4) reduces to the fitness model for undirected graphs. Finally, when all the in- and out-degrees of the nodes are taken as sufficient statistics, that is, $q = 2n$ and $f_i = d_i^{in}, f_{i+n} = d_i^{out}, i = 1, \ldots, n$, Eq. (4) reduces to the directed version of the fitness model of Eq. (3).

In the above setting, the fitnesses θs are given. In our (temporal) modeling approach below, they are promoted to random variables with a given probability distribution. Thus, the network metrics become random variables depending also on the latent variables θs and on their probability distribution $P(\vec{\boldsymbol{\theta}})$. Consider, for simplicity, an *undirected* network (the equations easily generalize to the directed case). The expected value of a network metric f is

$$\begin{aligned}\mathbb{E}[f(\mathbf{A})] &= \int f(\mathbf{A})P(\mathbf{A}|\vec{\boldsymbol{\theta}})P(\vec{\boldsymbol{\theta}})\, d\vec{\boldsymbol{\theta}} \\ &= \int f(\mathbf{A}) \prod_{i>j} P(a_{ij}|\theta_i, \theta_j)p_{\vec{\theta}}(\theta_i, \theta_j)\, d\vec{\boldsymbol{\theta}},\end{aligned} \tag{5}$$

where $p_{\vec{\theta}}$ is the bivariate probability density function of (θ_i, θ_j). Considering it as an important example in the following network density of Eq. (1), this expression simplifies to

$$\mathbb{E}[\delta] = \frac{2}{n(n-1)} \sum_{i>j} \int_{-\infty}^{\infty} \int_{-\infty}^{\infty} \frac{1}{1+e^{-(\theta_i+\theta_j)}} p_{\vec{\theta}}(\theta_i, \theta_j)\, d\theta_i\, d\theta_j. \quad (6)$$

In view of the dynamical model we are going to present below, we explicitly consider the case when $p_{\vec{\theta}}(\theta_i, \theta_j)$ is a bivariate Gaussian where the two variables have mean m_i and m_j, respectively, the same variance s^2, and correlation coefficient r. In this case, there is no closed-form expression for the double integral in Eq. (6). However, with a change of variables, it can be expressed in terms of the logistic-normal integral

$$I(m, s^2) := \frac{1}{\sqrt{2\pi s^2}} \int_{-\infty}^{\infty} \frac{1}{1+e^{-x}} e^{-\frac{1}{2}\left(\frac{x-m}{s}\right)^2} dx, \quad (7)$$

which is widely used in Bayesian analysis and for which several approximations exist (see Demidenko, 2013). It is easy to show that, under the above Gaussian assumptions, it holds

$$\int_{-\infty}^{\infty} \int_{-\infty}^{\infty} \frac{1}{1+e^{-(\theta_i+\theta_j)}} p_{\vec{\theta}}(\theta_i, \theta_j)\, d\theta_i\, d\theta_j = I\left(m_i + m_j, 2s^2(1+r)\right).$$

These results can be used to find the average density when all θs have the same Gaussian marginal distribution $\mathcal{N}(m, s^2)$ and the correlation coefficient of each pair is r,

$$\mathbb{E}[\delta] = I(2m, 2s^2(1+r)), \quad (8)$$

as a function of m, s, and r. These calculations are detailed in Appendix A.

As mentioned above, given its importance in statistics, there are several approximations of the function I when s is small. It is known that the first-order approximation performs poorly; so, in the following, we will use the second-order approximation (see Demidenko, 2013),

$$I(m, s^2) \approx \frac{1}{1+e^{-m}} \cdot \frac{1}{\sqrt{1+\frac{s^2 e^m}{(1+e^m)^2}}} \cdot e^{\frac{s^2}{2((1+e^m)^2+s^2 e^m)}}. \quad (9)$$

Figure 1 shows the comparison between the exact solution of the logistic-normal integral by varying the parameters m and s. The plots show that the approximation level is very good for values of s smaller than the absolute mean $|m|$.

This result allows us to compute the expected density of an undirected network from a fitness model with homogeneous Gaussian distributed θs, i.e., when $P(\vec{\boldsymbol{\theta}})$ is a multivariate Gaussian distribution with $\mathbb{E}[\theta_i] = m$, $Var[\theta_i] = s^2$, and $Cor[\theta_i, \theta_j] = r$, $\forall i, j = 1, \ldots, n$, as

$$\mathbb{E}[\delta] \approx \frac{1}{1+e^{-2m}} \cdot \frac{1}{\sqrt{1+\frac{2s^2(1+r)\,e^{2m}}{(1+e^{2m})^2}}} \cdot e^{\frac{2s^2(1+r)}{2((1+e^{2m})^2+2s^2(1+r)\,e^{2m})}}. \quad (10)$$

To shed more light on this result, we perform a Taylor expansion of around $s = 0$ of the right-hand side of Eq. (10),

$$\mathbb{E}[\delta] \approx \frac{1}{1+e^{-2m}} + (1+\rho)\frac{e^{2m}(1-e^{2m})}{(1+e^{2m})^3} s^2 + O(s^4). \quad (11)$$

When $s \to 0$, one obtains the expected density of an Erdös–Renyi model with $p = (1+e^{-2m})^{-1}$. However, for finite s, the density depends not only on the expected value of θ (i.e., m) but also on its variance and correlation. In particular, when $m < 0$ ($m > 0$), the expected density increases (decreases) with the variance s^2. This effect is amplified by larger correlation coefficients r.

Temporal network model. We now consider a temporal network $\mathcal{G}$ over the time snapshots $\mathcal{T} = \{1, \ldots, T\}$ constructed of unweighted networks G_t, $t \in \mathcal{T}$. The fitness model can be extended to the temporal networks domain by promoting the latent variables vector $\vec{\boldsymbol{\theta}}$ to dynamical variables. Specifically, for each time $t \in \mathcal{T}$, in an undirected temporal network, each node i is equipped with a latent variable $\theta_{i,t}$, representing its propensity to create links at time t, whereas, in the directed case, for each time $t \in \mathcal{T}$, each node i is equipped with a couple of latent variables $(\theta^{in}_{i,t}, \theta^{out}_{i,t})$ representing their propensity to create in and out arcs at time t, respectively. The latent state of the network is described by the vector $\vec{\boldsymbol{\theta}}_t \in \mathbb{R}^n$ (or $\mathbb{R}^{2n}$ in the directed case) collecting all latent variables. Analogously to the static case, these variables are used to generate the network using a link function. The probability that two nodes are linked by a link/arc

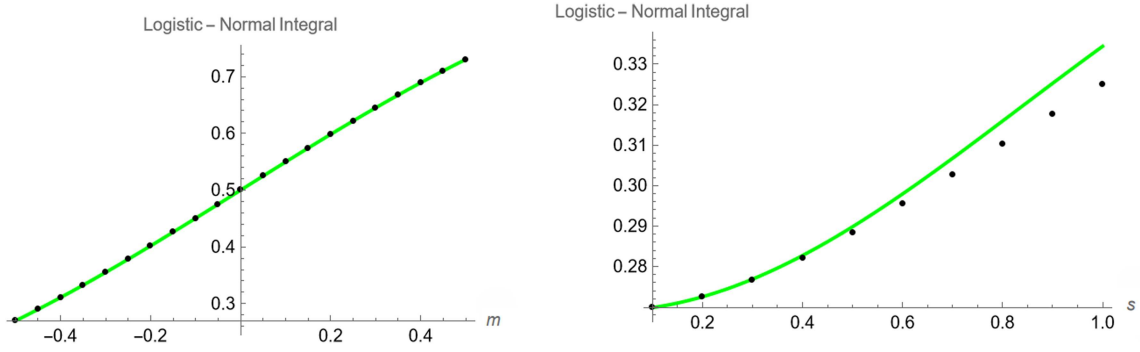

FIG. 1. Comparison between exact solution (dotted black line) and second-order approximation of the logistic-normal integral (green solid line) in Eq. (9). Parameters: $m = -0.5$, $s = 0.1$, $r = 0$. (Left) Comparison with respect to parameter m. (Right) Comparison with respect to parameter s.

at time t is given by a logistic function

$$g(\theta_{i,t},\theta_{j,t}) = P(a_{ij,t}=1|\theta_{i,t},\theta_{j,t}) = \frac{1}{1+e^{-\theta_{i,t}-\theta_{j,t}}} \quad \forall i,j\in V,\ \forall t\in\mathscr{T} \tag{12}$$

for the undirected network and

$$g(\theta^{out}_{i,t},\theta^{in}_{j,t}) = P(a_{ij,t}=1|\theta^{out}_{i,t},\theta^{in}_{j,t}) = \frac{1}{1+e^{-\theta^{out}_{i,t}-\theta^{in}_{j,t}}} \ \forall i,j\in V,\ \forall t\in\mathscr{T} \tag{13}$$

for the directed network.

To complete the model, it is necessary to specify the dynamics of vector $\vec{\boldsymbol{\theta}}_t$. Mazzarisi *et al.* (2020) proposed a model where each component of $\vec{\boldsymbol{\theta}}_t$ evolves independently as an AR(1) process, while Di Gangi *et al.* (2022) and Campajola *et al.* (2022) used a more flexible score-driven specification to filter a misspecified dynamics, including the possibility of describing non-stationary network dynamics. Importantly, also in this case, each component of $\vec{\boldsymbol{\theta}}_t$ evolves independently.

Since we are interested in modeling the dependence structure between nodes, in this paper, we explicitly consider the case where each latent variable is affected not only by itself but also by other nodes' latent variables. In doing so, we capture the temporal behavior of the latent variables of each node by observing the mutual relationships between them. Specifically, in our model, the vector $\vec{\boldsymbol{\theta}}_t$ evolves following a vector autoregressive model of order 1 (VAR(1)):

$$\vec{\boldsymbol{\theta}}_t = \vec{\boldsymbol{\mu}} + \mathbf{B}\vec{\boldsymbol{\theta}}_{t-1} + \vec{\boldsymbol{w}}_t, \tag{14}$$

where, in the undirected case (For the directed network, $\vec{\boldsymbol{\mu}}$ and $\vec{\boldsymbol{w}}_t$ have $2n$ components while $\mathbf{B}$ is a $2n\times 2n$ matrix.), $\vec{\boldsymbol{\mu}}\in\mathbb{R}^n$ is the vector of constant intercept, $\mathbf{B}$ is a $n\times n$ constant matrix expressing the mutual relations among the latent variables, and $\vec{\boldsymbol{w}}_t\in\mathbb{R}^n$ is the vector of error terms assumed to be Gaussian zero mean white noises. The covariance matrix of $\vec{\boldsymbol{w}}_t$ is indicated with $\boldsymbol{\Sigma}$. As usual in VAR models, covariance stationarity of Eq. (14) is guaranteed when the spectral radius (i.e., the maximum of the absolute values of the eigenvalues) of $\mathbf{B}$ is strictly smaller than one.

Vector $\vec{\boldsymbol{\mu}}$ controls the unconditional mean value of the latent variables, and, thus, the temporal average of the degree of each node or its in- and out-degrees in a directed case. In fact, the steady-state (or, equilibrium state) of the fitness vector is $\vec{\boldsymbol{\theta}}_S \equiv \mathbb{E}[\vec{\boldsymbol{\theta}}_t] = (\mathbf{I}-\mathbf{B})^{-1}\vec{\boldsymbol{\mu}}$, where $\mathbf{I}$ is the identity matrix. The unconditional mean is also controlled by $\mathbf{B}$, which describes the lagged interactions between latent variables. In particular, the diagonal elements of $\mathbf{B}$ describe the temporal autocorrelations of the θs and, thus, the autocorrelation of degrees. The off-diagonal elements describe how the latent variable of a node at time t affects the latent variable of another node at time $t+1$; thus, they are related to the lagged cross correlations between degrees.

III. IMPULSE RESPONSE ANALYSIS AND SHOCK PROPAGATION

In this section, we propose a modification of the impulse response analysis to study how a shock to a node or to a group of nodes in a temporal network propagates to other nodes and how the system relaxes back to its equilibrium state. Differently from other approaches that consider a shock on a network observable (e.g., a link disappears), we study shocks on nodes' characteristics by shocking the latent variables' dynamics.

In particular, we investigate the role of the model variables in determining the severity, breadth, and resilience of a shock.

The idea of considering the effect of a shock on a latent variable rather than on an observable variable (e.g., a link) can be motivated in the following way. First, latent variables often correlate with node-specific quantities and are more directly affected by shocks. For example, Mazzarisi *et al.* (2020) show that the fitness model estimations $e^{\theta^{out}_{i,t}}$ and $e^{\theta^{in}_{i,t}}$ in the unweighted interbank network highly correlate with the contemporaneous bank exposure, i.e., the amounts lent and borrowed, respectively, by bank i at time t. Thus, a shock $\theta^{out}_{i,t}\to\theta^{out}_{i,t}+\Delta$ corresponds to a log change of Δ in the amount lent by the bank (or, for small shocks, a $100\cdot\Delta\%$ change in the exposure). Similarly, in zero-inflated gravity models of the World Trade Web (Winkelmann, 2008 and Burger *et al.*, 2009), the probability of a trading link between countries i and j is

$$P(a_{ij}=1) = \frac{\overline{GDP_i}\cdot\overline{GDP_j}}{1+\overline{GDP_i}\cdot\overline{GDP_j}},$$

where $\overline{GDP_i}$ is the (suitably normalized) GDP of country i. Thus, we can identify $\theta_i = \log\overline{GDP_i}$ and a shock on θ_i corresponds to a log change of GDP equal to Δ. Therefore, a shock of a latent variable (i) is able to model a shock on a node rather than on a link and (ii) captures a possible shock in a node's intrinsic properties which drive the propensity in creating links.

The second reason for preferring shocks on nodes rather than on links can be econometrically motivated by the recent work of Di Gangi *et al.* (2022). This paper addresses the link prediction problem by comparing a Tobit regression model for a link at time t vs several observable network characteristics at previous times (Giraitis *et al.*, 2016) with a fitness-based approach, which forecasts the fitnesses of the nodes and, from them, predicts the link existence. The paper also shows that the latter approach outperforms the former, suggesting that to forecast future networks, it is better to use a lower dimensional representation of the network (with n fitnesses) rather than a much higher representation in terms of the n^2 observable links.

To be specific, we call $\tau\in\{0,\dots,T\}$ the time at which an exogenous shock, $\vec{\boldsymbol{\Delta\theta}}$, occurs in the vector $\vec{\boldsymbol{\theta}}_\tau$. In particular, we define a shock as a change in the state of vector $\vec{\boldsymbol{\theta}}$ from $\vec{\boldsymbol{\theta}}$ to $\vec{\boldsymbol{\theta}}+\vec{\boldsymbol{\Delta\theta}}$ at time τ. We define the (standard) Impulse Response Function (IRF) of the latent vector as

$$\boldsymbol{IRF}^{\vec{\boldsymbol{\theta}}}(t;\vec{\boldsymbol{\Delta\theta}}) = \mathbb{E}\big[\vec{\boldsymbol{\theta}}_{\tau+t}|\vec{\boldsymbol{\theta}}_\tau+\vec{\boldsymbol{\Delta\theta}},\vec{\boldsymbol{\theta}}_{\tau-1},\cdots\big] - \mathbb{E}\big[\vec{\boldsymbol{\theta}}_{\tau+t}|\vec{\boldsymbol{\theta}}_\tau,\vec{\boldsymbol{\theta}}_{\tau-1},\cdots\big], \tag{15}$$

where the expectation is taken over the realizations of noise $\vec{\boldsymbol{w}}_t$. As usual, this represents the expected marginal effect of the shock at time τ on the future value of the dynamical variable. (Note that in impulse response analysis, the shock is often applied to a component of the noise term, while here, we directly shock the latent variable.) We highlight that Eq. (15) shows the general formulation for the impulse response function of a dynamic system. By assuming

a VAR(1) as latent variables' dynamics in (14), due to the linearity of the VAR model, it is easy to verify (see Lütkepohl, 2005) that Eq. (15), in this case, reduces to

$$IRF^{\vec{\theta}}(t;\vec{\Delta\theta}) = \mathbf{B}^t\vec{\Delta\theta}, \tag{16}$$

which is, as expected, a linear function of the shock vector $\vec{\Delta\theta}$. Moreover, as well known in the theory of VAR processes, the IRF does not depend on $\vec{\theta}_\tau, \vec{\theta}_{\tau-1}\cdots$ but only on the shock vector $\vec{\Delta\theta}$ and on matrix $\mathbf{B}$.

However, we are interested in the expected marginal effect of shock on the properties of the observable network, which is a random function of vector $\vec{\theta}_t$. Thus, indicating with f a generic network metric at time t, we define the IRF of the metric of the temporal network as

$$\begin{aligned} IRF^{f}(t;\vec{\Delta\theta}) = {} & \mathbb{E}[f(\mathbf{A}_{t+\tau})|\vec{\theta}_\tau + \vec{\Delta\theta}, \vec{\theta}_{\tau-1}, \cdots] \\ & - \mathbb{E}[f(\mathbf{A}_{t+\tau})|\vec{\theta}_\tau, \vec{\theta}_{\tau-1}, \cdots], \end{aligned} \tag{17}$$

where the average is taken both on the noise of the VAR $\vec{w}_t$ and on the randomness generating the temporal networks, given the latent variables at each time.

We prove the following:

Proposition 1 *If $\vec{\theta}_t$ follows a VAR(1) dynamics, the impulse response function for the network metric f is*

$$\begin{aligned} IRF^{f}(t;\vec{\Delta\theta}) = {} & \int \mathbb{E}\left[f(\mathbf{A}_t)|\vec{\theta}_t\right] \\ & \cdot \left[\mathcal{N}\left(\vec{\theta}_t;\vec{\mu}_t + \mathbf{B}^{t-\tau}\vec{\Delta\theta}, \mathbf{\Sigma}_t\right) - \mathcal{N}\left(\vec{\theta}_t;\vec{\mu}_t, \mathbf{\Sigma}_t\right)\right] d\vec{\theta}_t, \end{aligned} \tag{18}$$

where

$$\vec{\mu}_t = (\mathbf{I}-\mathbf{B})^{-1}(\mathbf{I}-\mathbf{B})^{t-\tau}\vec{\mu} + \mathbf{B}^{t-\tau}\vec{\theta}_\tau, \tag{19}$$

$$\mathbf{\Sigma}_t = (\mathbf{I}-\mathbf{B}^2)^{-1}(\mathbf{I}-\mathbf{B}^2)^{t-\tau}\mathbf{\Sigma}, \tag{20}$$

are, respectively, the conditional mean and variance of $\vec{\theta}_t|\{\vec{\theta}\}_{0:\tau}$ and $\mathbf{I}$ is the $n \times n$ identity matrix.

The proof is presented in Appendix B. Proposition 1 highlights five important facts:

1. The expectation $\mathbb{E}\left[f(\mathbf{A}_t)|\vec{\theta}_t\right]$ refers to the *static* fitness model. Thus, if one is able to compute the properties of the static model, with a Gaussian integration, it is possible to obtain the IRF in response to a shock.
2. Even if $\mathbf{\Sigma}$ is diagonal, $\mathbf{\Sigma}_t$ is not (unless, of course, $\boldsymbol{B}$ is also diagonal). Thus, correlations arise at $t > 1$ if the θs do not evolve independently but influence each other in the VAR.
3. Differently from the standard linear VAR, the above IRF *does* depend on the state of the system at the time of shock $\vec{\theta}_\tau$. Thus, in our model, the current history of the network affects its reaction to shocks.
4. Differently from the IRF on the θs in Eq. (16), the IRF on the network metric is a *nonlinear function* of shock $\vec{\Delta\theta}$. Thus, doubling the shock amplitude generally does not lead to a doubling of the effect on the network metric.
5. Finally, when $t \to \infty$, assuming stationarity of the VAR model, it is

$$\vec{\mu}_t \to (\mathbf{I}-\boldsymbol{B})^{-1}\vec{\mu},$$

$$\mathbf{\Sigma}_t \to (\mathbf{I}-\boldsymbol{B}^2)^{-1}\mathbf{\Sigma},$$

i.e., as expected, they converge to the stationary value and, therefore, the shock is completely re-absorbed.

Clearly, it is interesting to investigate how different model parameters affect the amplitude of the initial shock and the speed (i.e., the resilience) with which the system returns to the stationary state. Since this, in general, depends on a very large number of parameters, in Sec. IV, we consider a simple and analytically solvable setting.

IV. IMPULSE RESPONSE FUNCTION OF THE MEAN-FIELD MODEL

The dynamics of the VAR model in Sec. II and, therefore, of the IRF in Sec. III strongly depends on the structure of matrix $\mathbf{B}$. In the following, we consider different specifications, in the attempt of balancing flexibility with tractability. Matrix $\mathbf{B}$ depends, in fact, on n^2 or $4n^2$ parameters for undirected and directed networks, respectively, and some restrictions, both in modeling and in estimation, are in order.

The simplest setting is the one where all diagonal elements of $\mathbf{B}$ are equal to $a \in \mathbb{R}$ and all off-diagonal elements are equal to $b \in \mathbb{R}$. When the components of $\vec{\mu}$ and the variance of noise are also equal to the vanishing covariances, i.e., $\mathbf{\Sigma} = \sigma^2\mathbf{I}$, we have a sort of "mean-field" setting, where all nodes are statistically equivalent and equally affected by all the other nodes. The largest eigenvalue of matrix $\mathbf{B}$ is $\lambda_1 = a + b(n-1)$ and covariance stationarity of the VAR model is guaranteed when $|\lambda_1| < 1$. The stationary value of $\vec{\theta}$ is

$$\vec{\theta}_S = \frac{\mu}{1-\lambda_1}\vec{1}, \tag{21}$$

i.e., all θs, on average, have the same value.

A slightly more sophisticated setting assumes that not all the off-diagonal elements of $\mathbf{B}$ are non-vanishing. This describes a situation where the (lagged) interactions are sparse and the dynamics of the latent variable of a node depends only on a subset of other nodes. The model is characterized by an extra parameter p giving the probability with which a non-diagonal element of $\mathbf{B}$ is different from zero and equal to b. Note that this extra stochasticity is quenched, i.e., matrix $\mathbf{B}$ is the same at all time steps. Clearly, when $p \to 1$, this model coincides with the mean-field one described above, while for $p \to 0$, only self-interactions are present, reducing the VAR model to a series of n AR(1) processes similar to Mazzarisi *et al.* (2020).

It is interesting to note that, when, as in the sparse or dense mean-field model, it is $\vec{\mu} = \mu\vec{1}$, then

$$\vec{\theta}_S = (\mathbf{I}-\mathbf{B})^{-1}\vec{\mu} = \mu(\mathbf{I}-\mathbf{B})^{-1}\vec{1}, \tag{22}$$

i.e., the stationary value of the fitness of a node is its Katz centrality when the VAR matrix $\mathbf{B}$ is seen as an adjacency matrix of a weighted network. The Katz centrality (Katz, 1953) depends on a tuning parameter α, which in Eq. (22) is set equal to 1. Since the

largest eigenvalue of $\mathbf{B}$ is smaller than 1, the condition $1 = \alpha < \lambda_1^{-1}$ is automatically satisfied for stationary VAR. This interesting result shows that the most central nodes in the interaction network (having $\mathbf{B}$ as the weighted adjacency matrix) are the ones with the largest degree in the observed stationary network (having $\mathbf{A}$ as the adjacency matrix)

In this section, we derive analytically the IRF in Eq. (18) for an undirected (for the sake of simplicity and clarity, we focus on an undirected network but, by simple calculations, it is also possible to derive the IRF for a directed network) network at any time t by considering as a property the network density, i.e., $f = \delta$ defined in Eq. (1). As said above, the $\boldsymbol{IRF}^f(t; \vec{\boldsymbol{\Delta\theta}})$ of Eq. (18) depends on the state of system $\vec{\boldsymbol{\theta}}_\tau$, at the time of the shock τ. Specifically, we assume to work in the mean-field setting and that the fitness of node (Note that in this homogeneous framework, the choice of the shocked fitness does not influence the IRF. We select the first node for simplicity.) $i = 1$ is shocked at time $\tau = 0$ by an amount Δ, i.e., $\vec{\boldsymbol{\Delta\theta}} = (\Delta, 0, \ldots, 0)'$ so that $\vec{\boldsymbol{\theta}}_{\mathbf{0}} \to \vec{\boldsymbol{\theta}}_{\mathbf{0}} + \vec{\boldsymbol{\Delta\theta}}$. To get an intuition on the role of the model's parameters, we consider the case when just before the shock, all θs have the same value. Of course, one could choose it equal to the stationary value θ_S derived above, but then, we will keep it general in order to study how the impulse response function depends on the initial state of the system.

The impulse response function in (18) depends on the dynamics of the conditional mean and variance of the fitness variables in Eqs. (19) and (20), respectively. In Appendix C, we show that the conditional mean and variance can be written in terms of parameters a, b and of the spectral radius as

$$\vec{\boldsymbol{\mu}}_t = \left(\frac{1-(a-b)^t}{1-(a-b)}\mathbf{I} + \left[\frac{1-\lambda_1^t}{1-\lambda_1} - \frac{1-(a-b)^t}{1-(a-b)}\right]\frac{1}{n}\mathbf{1}\right)\vec{\boldsymbol{\mu}} + \left((a-b)^t\mathbf{I} + \frac{\lambda_1^t-(a-b)^t}{n}\mathbf{1}\right)\vec{\boldsymbol{\theta}}_0 \tag{23}$$

and

$$\boldsymbol{\Sigma}_t = \left(\frac{1-(a-b)^{2t}}{1-(a-b)^2}\mathbf{I} + \left[\frac{1-\lambda_1^{2t}}{1-\lambda_1^2} - \frac{1-(a-b)^{2t}}{1-(a-b)^2}\right]\frac{1}{n}\mathbf{1}\right)\boldsymbol{\Sigma}, \tag{24}$$

where $\mathbf{1}$ is all-ones matrix, i.e., a matrix whose elements are one.

As already stated in Sec. II, it is immediate to observe two facts: (i) for $t \geq 2$, the matrix $\boldsymbol{\Sigma}_t$ is no longer diagonal and (ii) the shock intensity does not influence the conditional variance of the fitness variables $\boldsymbol{\Sigma}_t$. Regarding the first point, we label by $\sigma_t = \Sigma_{ii,t}$ and $\rho_t = \Sigma_{ij,t}/\Sigma_{ii,t}$ the conditional variance and the correlation coefficient of each node, respectively. As for the second point, the shock intensity Δ influences the conditional mean of the fitness variables and indicating $\vec{\boldsymbol{\mu}}_t^s = \vec{\boldsymbol{\mu}}_t + \mathbf{B}^t\vec{\boldsymbol{\Delta\theta}}$, one obtains

$$\vec{\boldsymbol{\mu}}_t^s = \left(\frac{1-(a-b)^t}{1-(a-b)}\mathbf{I} + \left[\frac{1-\lambda_1^t}{1-\lambda_1} - \frac{1-(a-b)^t}{1-(a-b)}\right]\frac{1}{n}\mathbf{1}\right)\vec{\boldsymbol{\mu}} + \left((a-b)^t\mathbf{I} + \frac{\lambda_1^t-(a-b)^t}{n}\mathbf{1}\right)\left(\vec{\boldsymbol{\Delta\theta}} + \vec{\boldsymbol{\theta}}_0\right). \tag{25}$$

The entries of $\vec{\boldsymbol{\mu}}_t^s$ in (25) can have different dynamics. Indeed, once the shock is triggered, node 1 is directly shocked and all the other nodes are shocked indirectly through node 1. We label z, the generic neighbor of node 1. We indicate the conditional mean of the shocked node by $\mu_{1,t}^s$, while the conditional mean of all other nodes z by $\mu_{z,t}^s$. They are defined as

$$\mu_{1,t}^s = \mu\left(\frac{1-(a-b)^t}{1-(a-b)} + \left[\frac{1-\lambda_1^t}{1-\lambda_1} - \frac{1-(a-b)^t}{1-(a-b)}\right]\frac{1}{n}\right) + \theta_0(a-b)^t + \frac{1}{n}(n\theta_0+\Delta)\left(\lambda_1^t-(a-b)^t\right) + \Delta(a-b)^t, \tag{26}$$

$$\mu_{z,t}^s = \mu\left(\frac{1-(a-b)^t}{1-(a-b)} + \left[\frac{1-\lambda_1^t}{1-\lambda_1} - \frac{1-(a-b)^t}{1-(a-b)}\right]\frac{1}{n}\right) + \theta_0(a-b)^t + \frac{1}{n}(n\theta_0+\Delta)\left(\lambda_1^t-(a-b)^t\right). \tag{27}$$

Equations (26) and (27) highlight that the difference between the conditional means is the term $\Delta(a-b)^t$, which expresses the impact of a shock t times after $\tau = 0$. In this framework, the impulse response function taking $f = \delta$ at any time $t \geq 0$ can be written explicitly in terms of the logistic-normal integral as

$$\boldsymbol{IRF}^\delta(t; \vec{\boldsymbol{\Delta\theta}}) = \frac{2}{n}I\left(\mu_{1,t}^s + \mu_{z,t}^s, 2\sigma_t^2(1+\rho_t)\right) + \frac{n-2}{n}I\left(2\mu_{z,t}^s, 2\sigma_t^2(1+\rho_t)\right) - I\left(2\mu_t, 2\sigma_t^2(1+\rho_t)\right). \tag{28}$$

The first term describes the effect on the density of the shocked node and the other nodes, while the second term describes the indirect effect on density due to the connections between non-shocked nodes. The last term is the baseline density when the shock is not present.

The immediate effect on the density is described by the above expression when $t = 1$. In this case, the IRF can be written as

$$\boldsymbol{IRF}^\delta(1; \vec{\boldsymbol{\Delta\theta}}) = \frac{2}{n}I\left(2\mu + 2\lambda_1\theta_0 + (a+b)\Delta, 2\sigma^2\right) + \frac{n-2}{n}I\left(2\mu + 2\lambda_1\theta_0 + 2b\Delta_0, 2\sigma^2\right) - I\left(2\mu + 2\lambda_1\theta_0, 2\sigma^2\right). \tag{29}$$

Finally, when we consider the model with the sparse VAR matrix, we will consider averages over different realizations of $\mathbf{B}$. This accounts to replace the off-diagonal elements of $\mathbf{B}$ with bp. This is due to the fact that when the elements of $\mathbf{B}$ are i.i.d. and we indicate with $\mathbb{E}[\mathbf{B}] = \bar{\mathbf{B}}$, then it is direct to show that $\mathbb{E}[\mathbf{B}^k] = \bar{\mathbf{B}}^k$.

A. Numerical analysis

To get an intuition on the role of the different model parameters on the relaxation dynamics of the network, we perform, in this section, a comparative statics using the results on the mean-field model presented in Sec. IV. As a baseline scenario, we consider a network of $n = 50$ nodes, and we choose $a = 0.3$ and $b = 0.01$, corresponding to a maximum eigenvalue $\lambda_1 = a + b \cdot (n-1) = 0.79$,

and we fix the noise variance $\sigma^2 = 0.1$. Then, we consider three values for parameter μ, $\mu \in \{-0.3, 0, 0.3\}$, corresponding to "sparse," "average," and "dense" networks, since the corresponding network densities are 0.05, 0.5, and 0.95, respectively. We assume that the fitness of all the nodes at the time of the shock are at the stationary value $\theta_{i,0} = \theta_S = \mu/(1 - \lambda_1)\ \forall i$, that is, $\theta_S \in \{-1.43, 0, 1.43\}$, and a shock intensity $\Delta = -10$. A negative value of Δ corresponds to a sudden drop in the fitness of the shocked node 1 and as a consequence of the density of the network. Finally, in all the computations, we use the second-order approximated value of I as in Eq. (9). Notice that all the computations in this section are analytical and follows from the expression derived above.

Shock intensity Δ. We first study the role of the shock intensity and, therefore, beyond the baseline case $\Delta = -10$, we also consider $\Delta = 10$ and $\Delta = -20$. Note that in the standard VAR model, the IRF is proportional to Δ [see Eq. (16)]; thus, it is expected to be symmetric for shocks with the same intensity but opposite sign. This is, indeed, also observed for the IRF on the density when $\mu = 0$, i.e., when the average network density is 0.5 [see panel (a) of Fig. 3]. However, when $\mu \neq 0$, a clear asymmetric pattern emerges [see Fig. 2 and panels (b) and (c) of Fig. 3]. Taking the dense network as an example [panel (b)], a shock of $\Delta = -10$ has an immediate negative effect on the density, which is three times larger than a positive shock of $\Delta = 10$. When the time elapses, the decay pattern in the two cases becomes more similar in absolute value. A symmetric behavior is observed for sparse networks [panel (c)]. This effect can be explained by noticing that when μ is positive (negative), the network density varies in absolute terms much more with negative (positive) shock than with positive (negative) one. This mirroring and asymmetric effect is explained by the presence of the positive (negative) μ, which increases (decreases) the network density with respect to 0.5. The higher (lower) the parameter μ, the higher (lower) the probability that two nodes are connected and, therefore, a positive (negative) μ will modify the network density negligibly because most of the nodes are already connected (disconnected). On the other hand, when Δ and μ have opposite signs, the network density changes significantly. The range of variation depends on μ and Δ. Finally, the non-linear relation between μ and Δ causes the system to react to shock differently both in terms of pattern and absorption time. The figure also shows the case $\Delta = -20$ and it is clear that, especially for short times, the pattern of the IRF is different from twice the pattern for $\Delta = -10$, pointing again at a non-linear behavior of the IRF. It is interesting to note that when μ and Δ have the same sign, the maximum (minimum) effect might

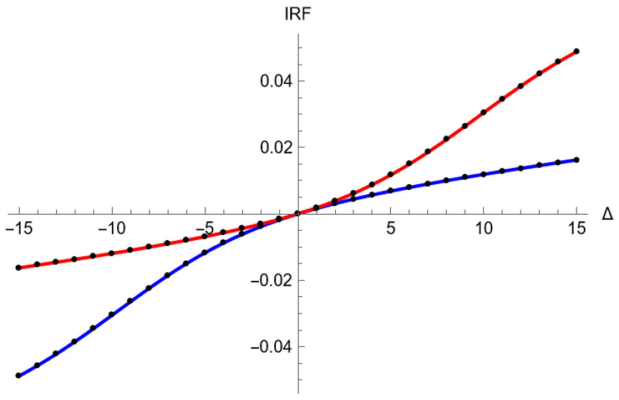

FIG. 2. Dependency of the IRF at time $t = 1$ with respect to Δ with $\mu = -0.3$ (red line) and $\mu = 0.3$ (blue line).

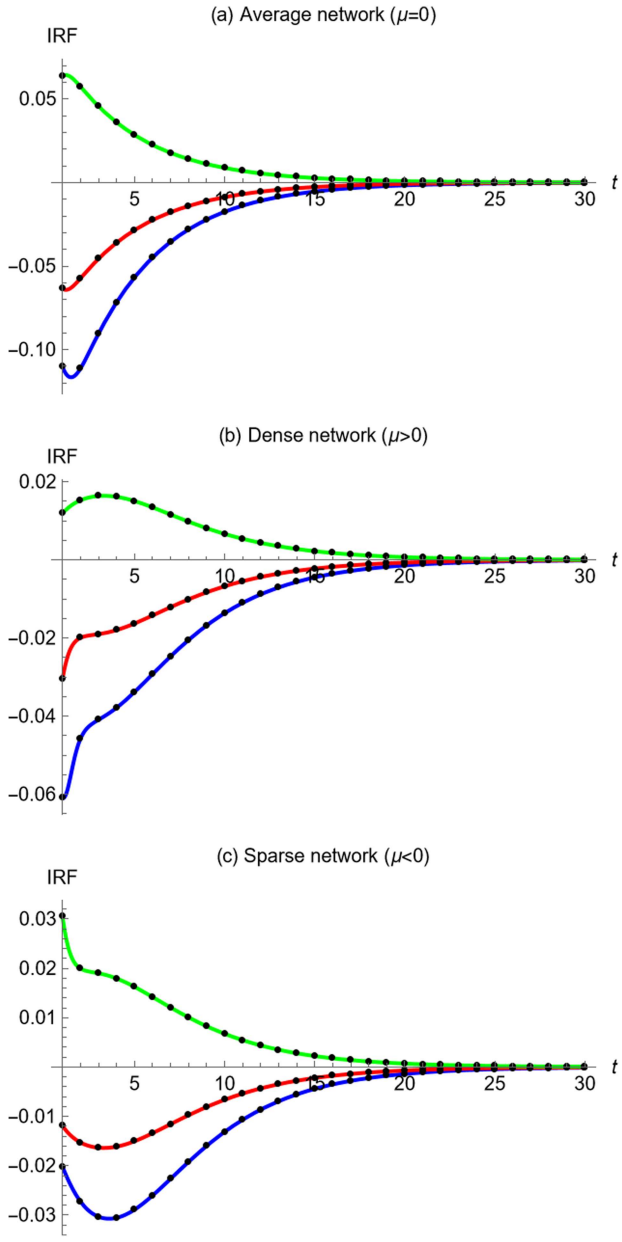

FIG. 3. Impulse response function with respect to Δ: $\Delta = -20$ (blue line), $\Delta = -10$ (red line), and $\Delta = 10$ (green line).

be reached at a time $t > 1$, while in the case of parameters with the opposite sign, the IRF is a strictly decreasing (increasing) function. We, therefore, conclude that in sparse networks, which are frequent in economic and financial applications, the larger disruption of a negative shock is expected to happen at a later time than the shock time.

Spectral radius of B. Since in the network case the IRF depends in a non-linear way on the powers of matrix **B**, it is interesting to assess the role of the spectral radius of **B** in Eq. (14) in shock spreading. We modify the spectral radius of matrix **B** by changing the parameters a and b such that $\lambda_1 \in \{0.69, 0.79, 0.89\}$. In particular, first, we modify the parameter a keeping the parameter $b = 0.01$ fixed, and later, we vary the parameter b keeping the parameter $a = 0.3$ fixed. In the first comparative statics, we set $a \in \{0.2, 0.3, 0.4\}$, while in the second comparative statics, we choose $b \in \{7.9592 \times 10^{-3}, 0.01, 1.2041 \times 10^{-2}\}$. Results are plotted in Figs. 4 and 5 both having the baseline as the middle case. Based on the linearity of the VAR model, we expect stronger and longer lasting effects of the shock when λ_1 is larger. This is, indeed, observed when $\mu = 0$ [panel (a) of Fig. 4]. In this case, the results suggest that the higher the spectral radius, the higher is the effect on the network density and the longer is the absorption time. [Indeed, by simple calculations, it is possible to notice that the IRF at time 1 depends only on the presence of parameter a in the first term of (29).] More interestingly, when $\mu \neq 0$ [panels (b) and (c) of Fig. 4], we observe the opposite effect at short times, i.e., the lower the spectral radius, the larger is the effect of the shock. However, the speed of relaxation is faster for smaller spectral radius, as expected. Regarding the shock effect, when $\mu \neq 0$, a change in λ_1 leads to a different equilibrium value of the fitness. By assuming a positive mean, the higher the value of a, the higher the spectral radius and the higher the equilibrium value (indeed, for $\mu > 0$ and $\lambda_1' < \lambda_1'' < \lambda_1'''$, the equilibrium value ordering is

$$\frac{\mu}{1-\lambda_1'} < \frac{\mu}{1-\lambda_1''} < \frac{\mu}{1-\lambda_1'''}.$$

In the case of $\mu < 0$, the previous ordering is reversed). Moreover, for sparse networks, the lower λ_1 is, the sooner the IRF attains its maximum effect. This lagged effect can be explained by noticing that, keeping b fixed, increasing a, each fitness will be influenced more by itself at the previous time than by the others, and, therefore, the shock requires more time to be transmitted between the fitness and to produce a relevant effect in the network.

On the contrary, comparing Figs. 4 and 5, it is possible to notice that the fitnesses' connectedness affects only the IRF in the short-term. This result clearly emerges in panel (a) of Fig. 5 at $t = 1$: the higher the connection between the fitnesses, the higher is the shock effect on the network and, therefore, the lower is the IRF. In fact, focusing on panel (a) of Figs. 5 and 4, we observe that parameter b plays an essential role in determining the IRF at the time immediately after the shock. In fact, in Fig. 4, it is shown that by placing $b = 0.01$, the IRFs are concentrated around the value -0.06. Using different values of b (and keeping a fixed), the IRFs are in a wider range $(-0.04, 0.07)$. In the other panels of Fig. 5, there are no relevant differences in the IRF confirming the predominant role of parameter μ in the resilience of the network.

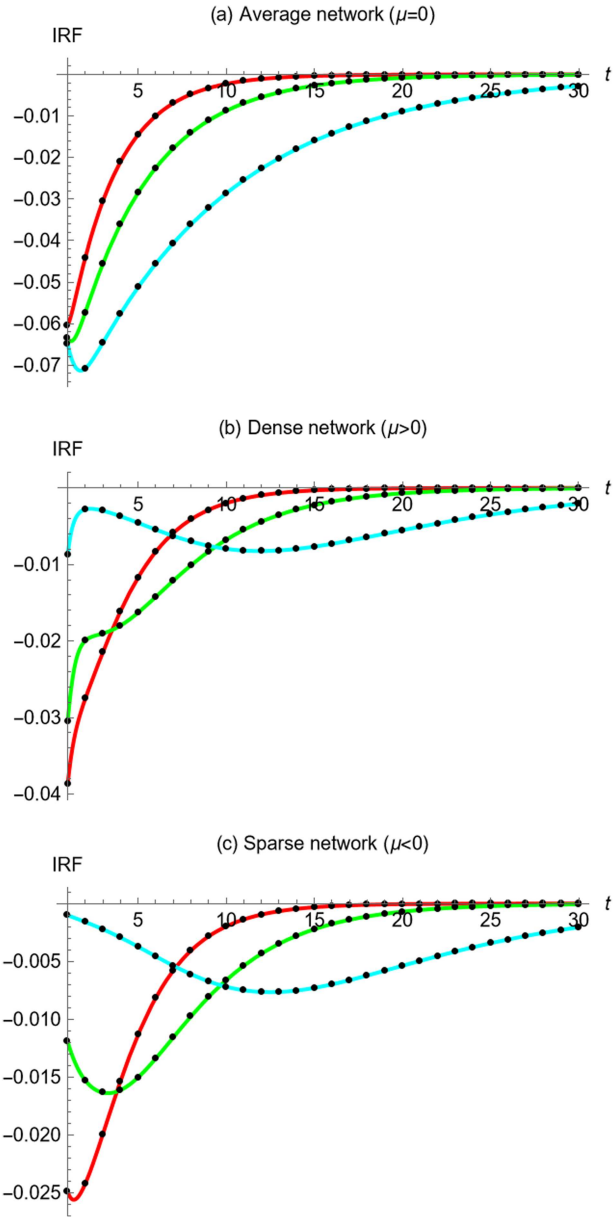

FIG. 4. Impulse response function with respect to a keeping $b = 0.01$: $a = 0.2$ (red line), $a = 0.3$ (green line), and $a = 0.4$ (cyan line).

Matrix B configuration. Although the spectral radius is an important determinant of the IRF's dynamics, it does not contain all the information on the role of **B**. Consequently, we investigate the role of parameters a and b in matrix **B** keeping the spectral radius constant to the baseline value $\lambda_1 = 0.79$. We consider three cases: (i) high cross-correlation and low autocorrelation, (ii) baseline scenario, and (iii) low cross-correlation and high autocorrelation. In

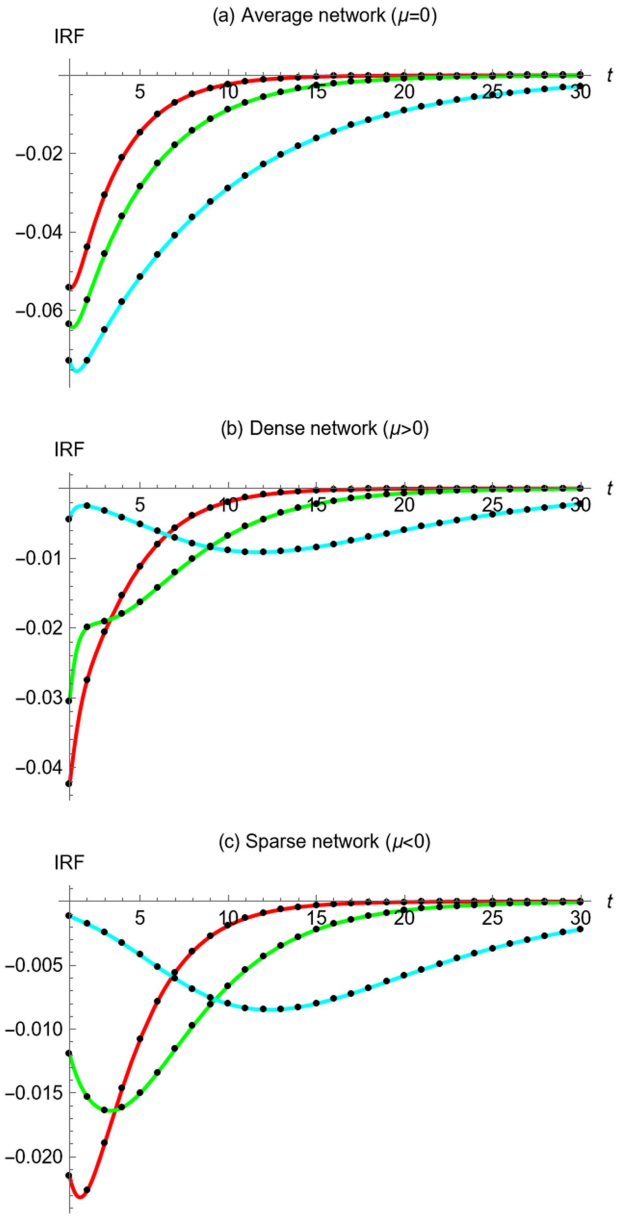

FIG. 5. Impulse response function with respect to b keeping $a = 0.3$: $b = 7.9592 \times 10^{-3}$ (red line), $b = 0.01$ (green line), and $b = 1.2041 \times 10^{-2}$ (cyan line).

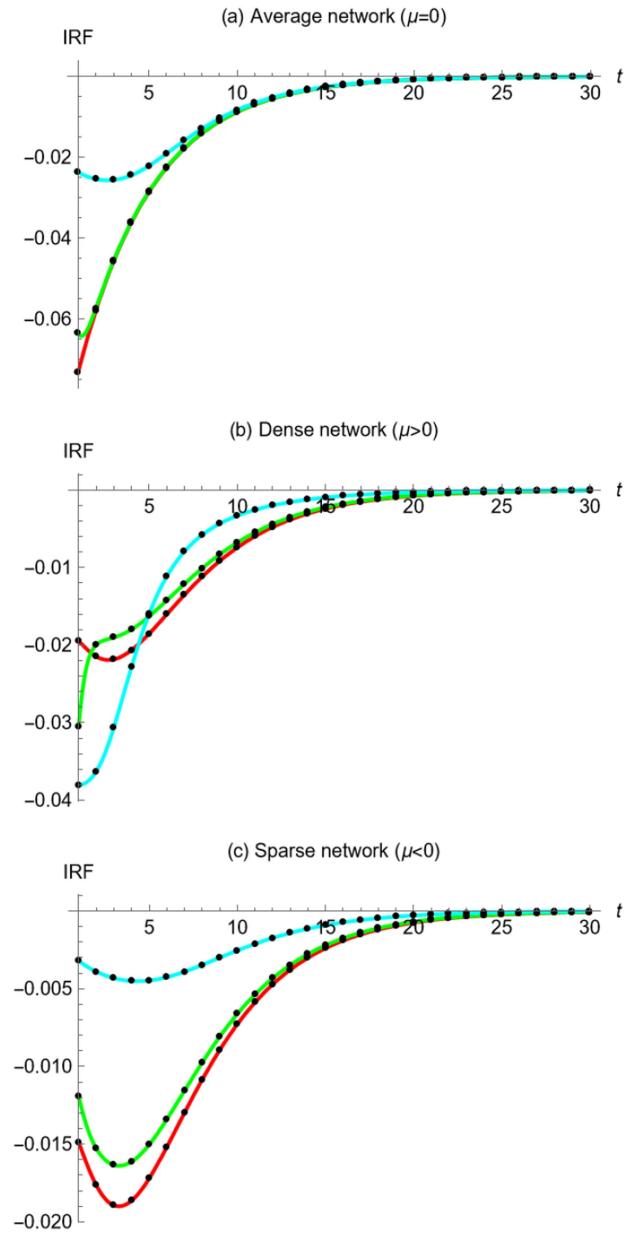

FIG. 6. Impulse response function with respect to a and b keeping $\lambda_1 = 0.79$: $a = 0.05$, $b = 1.5102 \times 10^{-2}$ (red line), $a = 0.3$, $b = 0.01$ (green line), and $a = 0.75$, $b = 8.1633 \times 10^{-4}$ (cyan line).

the first case, at any time t, $\vec{\theta}_t$ does not depend on its past history but rather on the connections between each fitness. In the third case, $\vec{\theta}_t$ depends significantly on $\vec{\theta}_{t-1}$ rather than on the connection between fitness pairs. Case (ii) is an intermediate case. In the first case, the driver of the spectral radius is parameter b, expressing the cross-correlation between θs from $t-1$ to t, while in the third case, the driver of the spectral radius is the autocorrelation of each fitness variable. The last case can be seen as a proxy of independent fitnesses, i.e., matrix **B** becomes a diagonal matrix and the VAR framework reduces to n independent AR(1) processes. The results are shown in Fig. 6.

An interesting result is that it is not possible to establish an absolute dependency between the IRF and the parameters a and b, since the latter depends strongly on the value of μ, which mainly

controls the probability of the existence of a link through the link function g.

Starting from the case with $\mu = 0$ [panel (a)], it is possible to observe that the higher the connection between couples of θs, i.e., the higher the parameter b, the higher is the impact of the shock on the network, and, therefore, the lower is the IRF. This result is highlighted also by observing the value of the IRF at time 1 of the cyan curve. When $\mu > 0$, i.e., in the presence of a dense network, the previous ordering is reverse: the higher the parameter a, the higher is the shock effect on the network, and, therefore, the lower is the IRF. This result can be interpreted by observing that in a dense network, the effect on the connection among θs is negligible since the network is characterized by a high number of links and the presence of additional links (due to the increase of b) does not significantly affect the IRF. On the contrary, when μ is negative, the highest impact happens when the fitnesses are (almost) fully connected, i.e., when b assumes a large value. Interestingly, it is possible to notice that an increase in parameter b translates to an increasing rate of the connection between the latent variables and, therefore, to the paths' weights through which a shock can be transmitted. Indeed, if we see matrix $\mathbf{B}$ as the adjacency matrix of a weighted graph, it is easy to observe that the higher b is, the higher the link weight, and, therefore, the higher the weight of shorter paths connecting the shocked node and all the other ones. This also explains why in Fig. 6 the impulse response function reaches its maximum at $t \geq 1$.

Noise level σ^2. Let us recall that the standard IRF in the VAR framework depends only on the power of matrix $\mathbf{B}$ and on the shock intensity $\vec{\mathbf{\Delta}}$. As mentioned in Sec. III, in the network case, the IRF depends also on the noise variance σ^2 of the θs. Therefore, we perform a comparative static of the IRF with respect to parameter σ^2 as $\sigma^2 \in \{0.01, 0.1, 0.5\}$. In the average network [panel (a) of Fig. 7], we observe that in the short-run, larger σ^2 leads to smaller effect on the network density. Therefore, the lower the parameter σ^2, the larger is the time needed, for the system to relax back to the equilibrium value. In the cases of dense and sparse networks, we observe an opposite behavior, since in the short-run, the deepest IRF is associated to the highest σ^2. The main driver of this behavior is μ. To show this, we study the IRF at time $t = 1$ by varying μ and choosing three values for σ^2. The result, displayed in Fig. 8, shows the existence of two thresholds $\underline{\mu} < 0$ and $\bar{\mu} > 0$, which define sparse and dense network cases, respectively. Notice that the thresholds are model parameters' driven: with the parameters of Sec. IV A, when $\mu \leq \underline{\mu}$, the network density is lower than 0.2, while for $\mu \geq \bar{\mu}$, the network density is higher than 0.9. Figure 8 illustrates that if $\mu \in (\underline{\mu}, \bar{\mu})$, the IRF decreases when parameter σ^2 increases, whereas the opposite occurs when $\mu \notin (\underline{\mu}, \bar{\mu})$. We note that the interval $(\underline{\mu}, \bar{\mu})$ is not symmetric with respect to $\mu = 0$ highlighting the asymmetry that characterized the IRF (as seen also in Fig. 3) as well as the predominant role of parameter μ in shock spreading. Finally, we notice that panels (b) and (c) in Fig. 7 belong to the extreme cases since the network density is $\delta = 0.95$ [panel (b)] and $\delta = 0.05$ [panel (c)].

Initial condition $\vec{\boldsymbol{\theta}}_0$. Finally, we perform a comparative statics of the IRF by assuming that $\vec{\boldsymbol{\theta}}_0 \neq \vec{\boldsymbol{\theta}}_S$. As done in the previous analysis, we consider three cases: $\mu \in \{-0.3, 0, 0.3\}$ so that $\theta_S \in \{-1.43, 0, 1.43\}$ and $\theta_{i,0} \in \{-0.75, 0, 0.75\}$ $\forall i$. Figure 9 shows that, surprisingly, it is not possible to identify a clear pattern for the

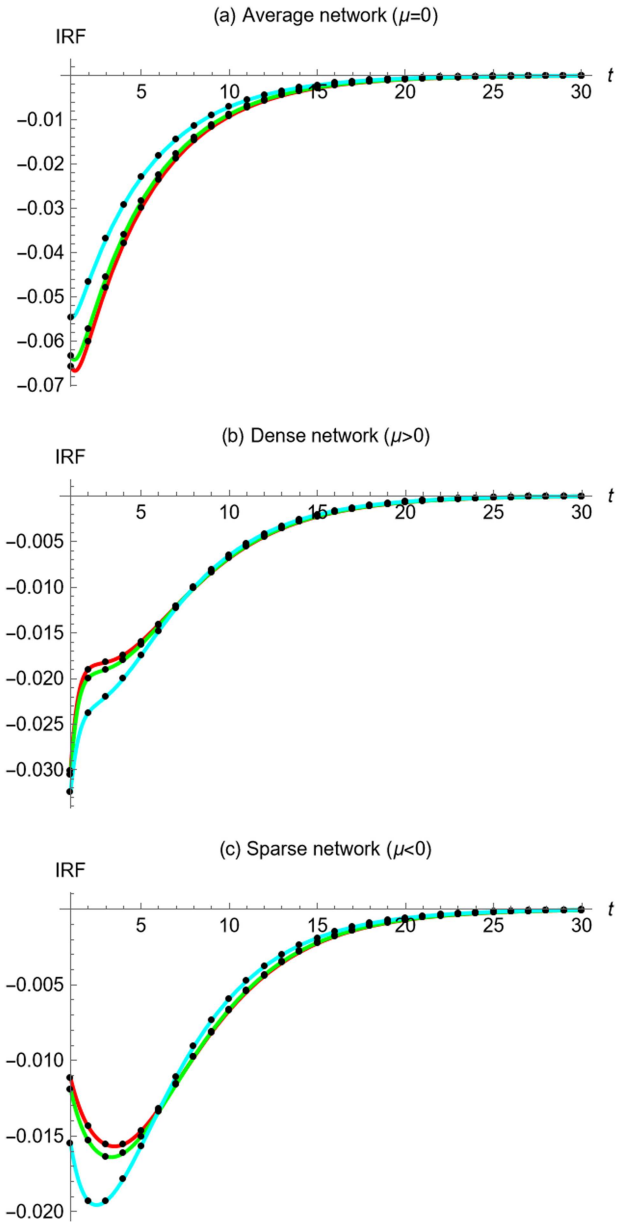

FIG. 7. Impulse response function with respect to σ^2: $\sigma^2 = 0.01$ (red line), $\sigma^2 = 0.1$ (green line), and $\sigma^2 = 0.5$ (cyan line).

dynamics of the IRF. Indeed, the time needed by the system to relax back to the equilibrium depends mainly on (i) the value of the system at the shock time, (ii) the parameter μ, and (iii) the sign of the shock. Intuitively, one can argue that the greater the distance between $\theta_{i,0}$ and $\theta_{i,S}$, the more time the system needs to relax back to equilibrium. This is partly true: however, the difference $|\theta_{i,0} - \theta_{i,S}|$ is not the only aspect to consider as the signs of Δ and θ_0's are also essential, as discussed extensively in this section. Indeed, concordant signs imply a

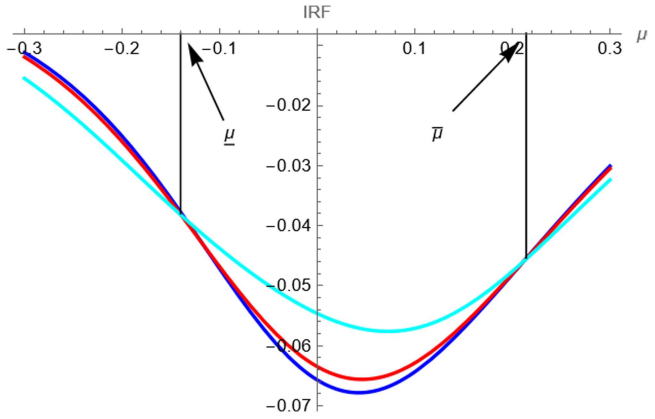

FIG. 8. Impulse response function at time 1 with respect to μ varying σ^2: $\sigma^2 = 0.01$ (red line), $\sigma^2 = 0.1$ (green line), and $\sigma^2 = 0.5$ (cyan line).

more moderate impact on δ rather than the case in which Δ and θ_0 have opposite signs. This last sentence can be observed by looking at the cyan line in panel (c) in Fig. 9.

V. MODEL ESTIMATION AND EMPIRICAL APPLICATION TO THE INTERBANK MARKET

In this section, we first introduce and discuss our novel heuristic estimation procedure of the model described above, showing its effectiveness with numerical simulations, and then, we present an empirical illustration to the dynamics of the Italian interbank network e-MID.

A. Estimation procedure

With the aim of applying the methodology developed in Sec. III to a real world application, the first issue relates to the estimation of fitness dynamics. Indeed, while exponential random graphs are extremely flexible and adaptable to numerous applications, one of the main problems faced by researchers deals with the estimation procedure since the latent variables are latent and not observable. Therefore, in this section, we propose a novel estimation procedure for temporal networks induced by latent variables' dynamics. Our approach is based on two steps: first, we estimate the fitness parameters by applying the Maximum Likelihood Estimation (MLE) procedure for each time period. However, despite that the MLE has been studied, and several algorithms have been implemented, Chatterjee *et al.* (2011) highlight that the procedure does not guarantee consistent estimates in the presence of sparse networks, such as the interbank network (see also Mazzarisi and Lillo, 2017). Additionally, the MLE method produces static estimations, that is, the likelihood function is maximized at each time, without considering the entire dynamics of $\vec{\boldsymbol{\theta}}_t$, i.e., regardless of the information embedded in the past values of θs. This approach is also known as the Single Snapshot Inference (SSI).

For these reasons, we propose a novel estimation procedure based on the Kalman filter (see Khodarahmi and Maihami, 2023 for a review) of a state space model composed by an observation and a latent dynamics equation. We consider the MLE estimations as noisy observation of the latent parameters, which follows the VAR dynamics described above.

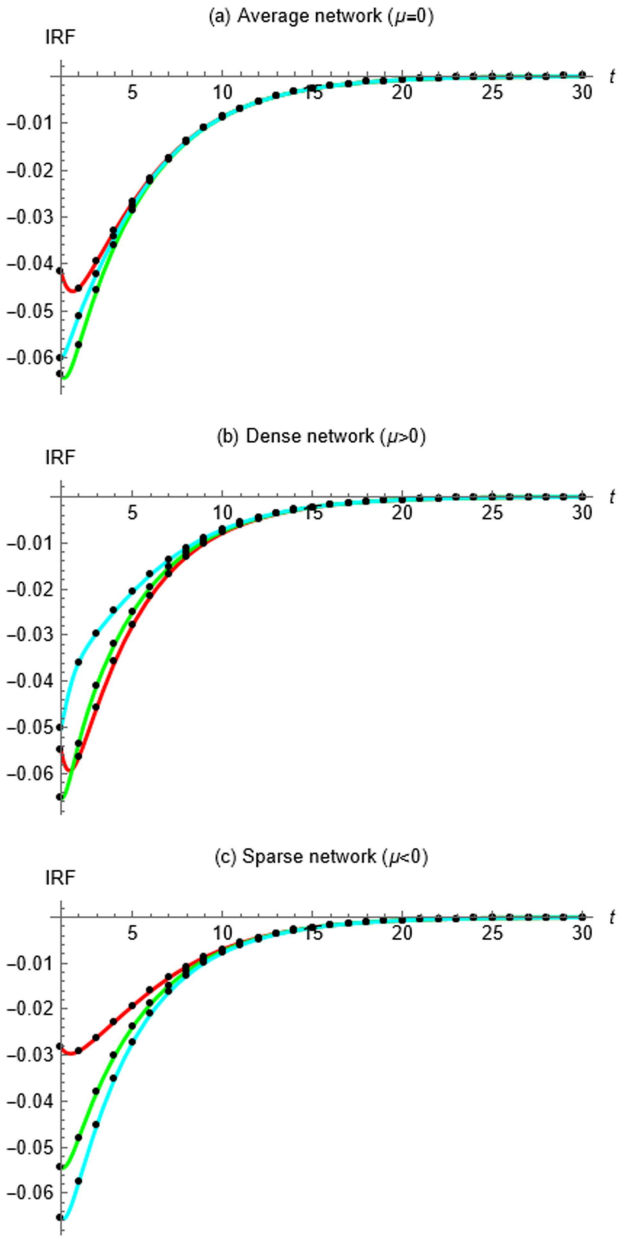

FIG. 9. Dependency of IRF on parameter μ choosing $\theta_0 = -0.75$ (red line), $\theta_0 = 0$ (green line), and $\theta_0 = 0.75$ (cyan line).

We remind that the MLE estimations $\vec{\boldsymbol{\Theta}}_t$ obtained by single snapshots and defined as

$$\vec{\boldsymbol{\Theta}}_t \in \arg\max P\left(\mathbf{A}_t | \vec{\boldsymbol{\theta}}_t\right) \tag{30}$$

are obtained as a solution of the system of nonlinear equations

$$\sum_{i\neq j} \frac{1}{1+e^{-\Theta_{i,t}-\Theta_{j,t}}} = d_{i,t}, \quad i \in V, \quad t \in \mathscr{T} \tag{31}$$

in the undirected case and

$$\sum_{i<j} \frac{1}{1+e^{-\Theta^{in}_{i,t}-\Theta^{out}_{j,t}}} = d^{in}_{i,t}, \quad i \in V, \quad t \in \mathscr{T}, \tag{32}$$

$$\sum_{i<j} \frac{1}{1+e^{-\Theta^{out}_{i,t}-\Theta^{in}_{j,t}}} = d^{out}_{i,t}, \quad i \in V, \quad t \in \mathscr{T}, \tag{33}$$

in the directed case.

We assume that the observed $\vec{\Theta}_t$ are possibly biased noisy estimates of the latent fitnesses $\vec{\theta}_t$, i.e.,

$$\vec{\Theta}_t = \vec{\gamma} + \mathbf{I}\vec{\theta}_t + \vec{\nu}_t,$$

where $\vec{\gamma}$ is a constant vector, $\vec{\theta}_t$ is the vector collecting the unbiased estimation of the fitness vector, and $\vec{\nu}_t$ is a zero mean Gaussian vector with a constant covariance matrix. The latent state dynamics is described by VAR(1) as in Eq. (14). Therefore, the state space model is described by the following system of equations:

$$\begin{cases} \vec{\theta}_t = \vec{\mu} + \mathbf{B}\vec{\theta}_{t-1} + \vec{w}_t, \\ \vec{\Theta}_t = \vec{\gamma} + \mathbf{I}\vec{\theta}_t + \vec{\nu}_t, \end{cases} \tag{34}$$

which can be estimated with the Kalman filter. This procedure is termed the Kalman-Filter Single Snapshot Inference (KF-SSI). Section V B is devoted to checking the effectiveness of our estimation procedure.

B. Numerical simulation

We investigate the effectiveness of our estimation procedure presented in Sec. V A by performing numerical simulations of the fitness dynamics in Eq. (14). With the purpose of balancing flexibility and computational time, we assume to work in the mean-field framework as in Sec. IV. We compare the performance of the KF-SSI with the one obtained by performing MLE of the fitnesses, a procedure termed Naive Single Snapshot Inference (N-SSI). Our purpose is to show that KF-SSI achieves superior performances with respect to N-SSI in parameter estimation. We compare the two methods with the following steps:

1. Select the set of parameters $\vec{\Phi} = (\mu, a, b, \sigma^2)$.
2. Simulate n_{sim} time series for $\{\vec{\theta}_t\}_{t\in\mathscr{T}}$ according to dynamics (14).
3. Construct the network at each time t.
4. Apply the MLE procedure to estimate $\vec{\Theta}_t$ at each time t.
5. Estimate the parameters of the KF-SSI models and produce the latent state estimate mean at time t given observations up to and including at time t. For the N-SSI, we directly fit a VAR(1) model on the MLE fitnesses $\vec{\Theta}_t$ to obtain an estimate of the static parameters $\vec{\Phi}$.

TABLE I. The mean absolute relative error of the estimates of fitness dynamics and parameters of the network model.

	$\theta_{i,t}$	a	b	μ	σ^2
N-SSI	0.57	0.605	0.009	0.311	0.375
KF-SSI	0.404	0.124	0.023	0.118	0.144

6. For each estimation method, compute the relative errors in parameters estimation as

$$RE_{\phi,k} = \frac{\hat{\phi}_k - \phi}{\phi}, \quad k \in \{N-SSI, KF-SSI\}, \quad \phi \in \vec{\Phi},$$

where $\hat{\phi}_k$ is the estimation of parameter ϕ in the kth model. We then compute the mean absolute error over the simulations.
7. Compute the mean absolute error for the estimated fitness dynamics. The mean is obtained by averaging the error over the nodes and the simulations.

We simulate $n_{sim} = 100$ undirected networks of $n = 10$ nodes for $t \in \{1, \ldots, 100\}$ times in the mean-field model with parameters $a = 0.7$, $b = 0.07$, $\sigma = 0.2$, and $\mu = -0.07$. The mean absolute errors are reported in Table I, which confirms that the procedure KF-SSI greatly outperforms N-SSI for all model parameters except for parameter b.

C. Data

In this section, we apply the proposed methodology to the Italian electronic market for interbank deposits (e-MID). The e-MID is an electronic market in the Euro Area where nodes (banks) extend loans to one another for a specified term and/or as collateral. The e-MID network has been extensively studied in the last 20 years both in the field of complex networks and economics/financial mathematics; see, just to name a few, Iori *et al.* (2006), Iori *et al.* (2008), Iori *et al.* (2015), Cimini *et al.* (2015), Mazzarisi and Lillo (2017), Barucca and Lillo (2018), and Mazzarisi *et al.* (2020). The dataset contains the daily credit transactions between banks, mostly based in Italy, from March 9, 2012 to February 27, 2015. Following the approach in Mazzarisi *et al.* (2020), we aggregate weekly the daily data to create a temporal interbank network. At each time, an arc between two banks i and j indicates that bank i extends a loan to bank j. In doing so, we model the e-MID by the use of a temporal series of unweighted and directed networks.

As already pointed out by Barucca and Lillo (2018), the e-MID network is characterized by a sharp decrease in both number of active banks and traded volume after 2012 as a result of European sovereign debt crisis and unconventional monetary measures issued by the European Central Bank. To have a stationary sample, we focus our analysis on the period of 40 weeks from January to October 2014. We select eight banks according to two criteria: (i) their cumulated in- and out-degrees in the time horizon period exceed a fixed threshold set to 100, (ii) for each time t, the induced subgraph (the induced subgraph of a graph $G = (V, E)$ is a graph formed by a subset of nodes of G, V', and all the edges in E that connect pairs of vertices in V') does not contain isolated nodes.

D. Empirical results

We now consider real data of the e-MID (directed) interbank market by relaxing the mean field assumption on the structure of matrix **B** [We highlight that when applied to empirical data, the model in Eq. (34) can handle cases where the nodes' degree are heterogeneous]. In doing so, we are able to model those different types of lagged interactions between banks.

Figure 10 reports the sign of the entries of matrix **B**'s estimation. We observe that a high heterogeneity characterizes the entries of **B** both in terms of sign and weight (in absolute value). Indeed, the average entry of matrix **B** is -0.034 while the standard deviation of the entries of **B** is 3.06. Moreover, around half of the entries are positive (134 elements out of 256) including diagonal elements. The heterogeneity in the estimated matrix **B** highlights three main facts: (i) the relations between the banks' connections (degrees) in the analyzed period are diverse, reflecting the heterogeneous behavior in lending and borrowing interbank loans; (ii) being so different from the matrix of the mean-field model, each fitness has a different long-term equilibrium value given by Eq. (21); and (iii) different shocked nodes may lead to different IRFs.

For this specific network, one can try to give an interpretation to each entry of matrix **B**. A positive value of the diagonal elements of **B**, associated with the couple $(\theta^{in}_{i,t}, \theta^{in}_{i,t+1})$ or $(\theta^{out}_{i,t}, \theta^{out}_{i,t+1})$, indicates the persistence in the propensity to lend/borrow from the bank i, confirming the results, for example, in Freixas and Rochet (2008), Kobayashi and Takaguchi (2018), and Mazzarisi *et al.* (2020). A negative value for the matrix element corresponding to the couple $(\theta^{out}_{i,t}, \theta^{out}_{j,t+1})$ indicates that a large propensity to lend to bank i at a time t leads to a small propensity to lending to bank j the following week. This might be seen as the effect of competition in the credit supply market between banks. Clearly, a positive value might be the effect of a global request for credit, which is persistent (as seen above) and satisfied by lenders i and j at different times. A similar interpretation holds for the matrix element of the couple $(\theta^{in}_{i,t}, \theta^{in}_{j,t+1})$ but for the market of credit demand. Finally, a positive value for the matrix element corresponding to the couple $(\theta^{in}_{i,t}, \theta^{out}_{j,t+1})$ indicates that a large propensity to borrowing of bank i at a time t is associated with a large propensity to lending of bank j in the next period. Part of this might be due to the fact that $\theta^{in}_{i,t}$ is persistent, so $\theta^{in}_{i,t+1}$ is also likely to be large, creating an opportunity for lending by bank j. A similar interpretation, but with opposite sign, could be given to the value of the matrix element corresponding to $(\theta^{out}_{i,t}, \theta^{in}_{j,t+1})$. Although these interpretations are tentative and should be validated with more structural models, their meaning in terms of lagged correlation between the propensity to lending/borrowing can be certainly given as they follow from the significance of the VAR coefficient.

Based on these observations, we computed the IRF by shocking the node with the largest out-fitness at time τ. Moreover, we compute the IRF conditional on different information sets. Specifically, we simulate 500 IRFs for the e-MID interbank network conditional on a shock $\Delta = -0.3$ on the out-fitness of the node which, during the fifth week, presents the maximum out-degree. From an economic point of view, this scenario considers the case when the large lender bank in the market significantly reduces the amount lent to the other banks. The mean IRF and the 10th and 90th percentiles across simulations are plotted in Fig. 11. To compare the simulations results, we assume that the fitnesses values at the shock time are provided by the KF-SSI model specification in (34).

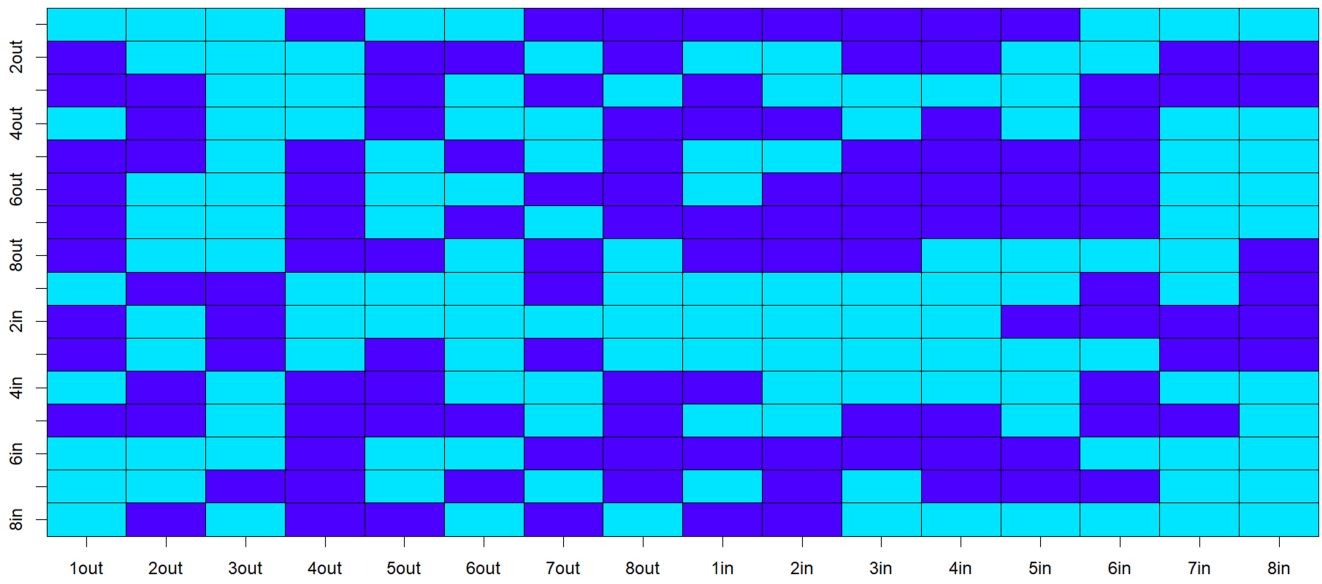

FIG. 10. Sign of the entries of matrix **B**. Dark blue and light blue entries refer to negative and positive elements, respectively. The ith row/column label shows the ith bank and direction (in or out).

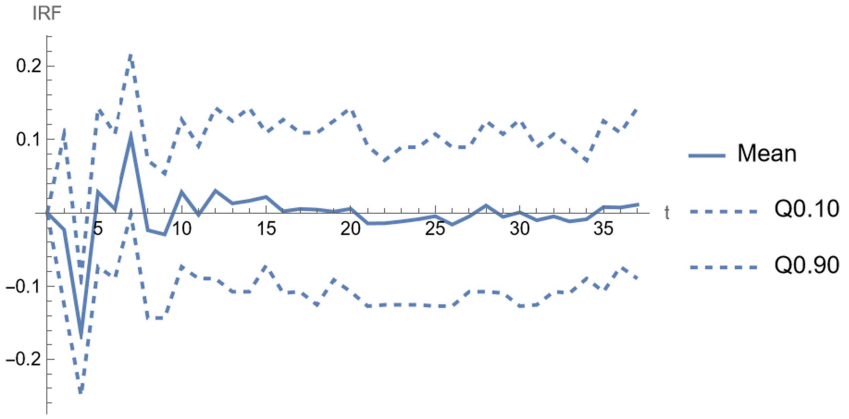

FIG. 11. Impulse response function for the e-MID network with negative $\Delta = -0.3$. The solid line represents the simulations' mean, dotted lines represent the 10th and 90th percentiles, respectively.

Interestingly, the largest negative variation occurs at a later time than $\tau + 1$, as already observed in the first comparative statics of Sec. IV A. This suggests that there exists a lagged effect in the shock spreading in the interbank market. Subsequently, the IRF presents a significant positive change, which leads the IRF to be positive. Finally, the shock is completely absorbed, and the network density relaxes back to the pre-shock value.

Finally, we study how the IRF depends on the network state at τ, i.e., on $\vec{\theta}_\tau$ and on the shocked node. To this end, we consider different initial conditions, as done also in Fig. 9 in Sec. IV A. We observe that in these cases, as already observed in Fig. 9, the IRF patterns are close to the one shown in Fig. 11. This result depends on three main factors: (i) on the VAR dynamics that we impose to $\vec{\theta}$'s in Eq. (14), (ii) the estimated fitness unconditional mean is negative, leading the network to be sparse, and (iii) the estimated volatility is low. Nevertheless, we observe a variation in the IRF depending on the shocked node: the higher the fitness value of the shocked node at the shock time, the lower the effect on the network density.

The presented approach has potential interest for policymakers and supervising authorities. Indeed, the results suggest that the dynamics of the IRF is mainly determined by matrix **B** of the VAR model. The estimation of such a matrix allows policymakers to assess the impacts of both systemic exogenous shocks and different economic/financial policies, especially, in the first case, knowing the entries of matrix **B** allows the policymaker to construct dynamic scenarios of the evolution of the interbank network under different stress conditions and possibly to minimize the effect of systemic risk.

VI. CONCLUSION

In this paper, we presented a dynamical model for temporal networks, and we introduced the first impulse response function for network metrics. The aim of the model and analysis is to assess how an external shock propagates in a temporal network, as well as to establish its resilience. This is done by extending the celebrated configuration or fitness model for a static network to a fully dynamical setting. The model associates each node to a pair of latent variables that represents its propensity to create in- and out-links in the network. We assume that these variables evolve stochastically in time according to a VAR(1) process to model the lead-lag relation between the linking propensities of the nodes. The consequence is that the network and all its metrics are stochastic. In such a framework, we analyze the variation of a given network metric after a shock in the fitness of a node. Additionally, we analyze how the system relaxes back to the equilibrium state, also examining the recovery time. We provide a general formulation for the IRF for a general network metric. We focus on the network density, and we derive a closed-form solution for its IRF under the assumption of fitnesses' homogeneity. To assess the role of each model's parameter, we make a comparative statics considering three different values for the network density corresponding to average, dense, and sparse networks. We propose an econometric approach to estimate the fitnesses' dynamics based on the Kalman filter. Finally, we apply our methodology to the e-MID network. The results highlight not only the different dynamics that characterize the lending/borrowing mechanism in the e-MID network but also specify the role of the banks in shock spreading, as well as the pattern through which a shock on the financial network is absorbed.

The presented framework can be extended in different directions. First, other types of networks could be considered, such as directed weighted networks. Moreover, other shock scenarios could be taken into account. Here, although we focused on a shock hitting a single node, one can easily extend our computations to the case when a subset or even all the nodes are simultaneously affected by a global shock. This would allow studying the shock propagation and resilience of a network when an exogenous shock hits a part of the system. Second, other network metrics can be investigated to understand the effect of shocks on their temporal evolution. Proposition 1 gives a general answer to the problem, but the detailed computations must be spelled out. Finally, it might be interesting to develop alternative and more rigorous estimation techniques that are able to infer the fitness dynamics in sparse networks. We leave these interesting questions for future research.

ACKNOWLEDGMENTS

This publication has received funding from the project "SoBigData.it—Strengthening the Italian RI for Social Mining and Big Data Analytics"—Prot. IR0000013—Avviso n. 3264 del 28/12/2021.

The research was carried out also with the contribution of the research groups linked to the European Program scheme "INFRAIA-01-2018-2019: Research and Innovation action," Grant Agreement No. 871042 "SoBigData++: European Integrated Infrastructure for Social Mining and Big Data Analytics."

AUTHOR DECLARATIONS

Conflict of Interest

The authors have no conflicts to disclose.

Author Contributions

Fabrizio Lillo: Conceptualization (equal); Data curation (equal); Formal analysis (equal); Funding acquisition (lead); Investigation (equal); Methodology (equal); Project administration (lead); Resources (equal); Software (equal); Supervision (lead); Validation (equal); Visualization (equal); Writing – original draft (equal); Writing – revised version (equal). **Giorgio Rizzini:** Conceptualization (equal); Data curation (equal); Formal analysis (equal); Investigation (equal); Methodology (equal); Resources (equal); Software (equal); Validation (equal); Writing – original draft (equal); Writing – revised version (equal).

DATA AVAILABILITY

The data that support the findings of this study can be obtained from the eMid market. The data are not publicly available due to privacy restrictions.

APPENDIX A: DERIVATION OF NETWORK DENSITY UNDER GAUSSIAN DISTRIBUTED FITNESSES

In this appendix, we show the passages to derive Formula (10). The case with different means is based on the same procedure. As stated in Sec. II, we assume that vector $\vec{\theta}$ is a multivariate Gaussian distribution whose entries all have the same mean m, variance s^2, and correlation factor r. We prove that the expected density of a network following a fitness model is

$$\begin{aligned}\mathbb{E}[\delta] &= \frac{1}{2s^2\pi\sqrt{1-r^2}}\int_{-\infty}^{\infty}\int_{-\infty}^{\infty}\frac{1}{1+e^{-(\theta_i+\theta_j)}} \\ &\quad\cdot e^{-\frac{1}{2s^2(1-r^2)}\left((\theta_i-m)^2-2r(\theta_i-m)(\theta_j-m)+(\theta_j-m)^2\right)}\,d\theta_i\,d\theta_j \\ &= I(2m, 2\sigma^2(1+r)), \end{aligned} \tag{A1}$$

where $I(2m, 2\sigma^2(1+r))$ is the normal-logistic integral. We first rearrange the numerator of the exponent inside the integral signs as

$$\begin{aligned}&(\theta_i-m)^2-2r(\theta_i-m)(\theta_j-m)+(\theta_j-m)^2 \\ &\quad= 2m^2-2\theta_j m-2\theta_i m-2m^2 r+\theta_i^2+\theta_j^2 \\ &\qquad-2\theta_i\theta_j r+2\theta_i mr+2\theta_j mr \\ &\quad= \theta_i^2+\theta_j^2-2m(\theta_i+\theta_j)+2mr(\theta_i+\theta_j) \\ &\qquad+r\left(\frac{-(\theta_i+\theta_j)^2}{2}+\frac{(\theta_i-\theta_j)^2}{2}\right)+2m^2(1-r) \\ &\quad= \frac{(\theta_i+\theta_j)^2+(\theta_i-\theta_j)^2}{2}-2m(\theta_i+\theta_j)(1-r) \\ &\qquad+r\left(\frac{-(\theta_i+\theta_j)^2}{2}+\frac{(\theta_i-\theta_j)^2}{2}\right)+2m^2(1-r), \end{aligned} \tag{A2}$$

where in the last passage, we use the fact that $\theta_i^2+\theta_j^2 = \frac{(\theta_i+\theta_j)^2+(\theta_i-\theta_j)^2}{2}$ and $-2\theta_i\theta_j = \frac{-(\theta_i+\theta_j)^2}{2}+\frac{(\theta_i-\theta_j)^2}{2}$.

Then, we use a change of variables $z = \theta_i - \theta_j$ e $w = \theta_i + \theta_j$ so that Eq. (A2) can be written as

$$\begin{aligned}&\frac{w^2+z^2}{2}-2mw(1-r)+r\left(-\frac{w^2}{2}+\frac{z^2}{2}\right) \\ &\quad+2m^2(1-r)++\frac{1}{2}z^2(1+r) \\ &\quad= \frac{1}{2}(w-2m)^2(1-r)+\frac{1}{2}z^2(1+r), \end{aligned}$$

and the double integral in Eq. (A1) can be written in terms of w and z as

$$\begin{aligned}&\frac{1}{2}\frac{1}{2s^2\pi\sqrt{1-r^2}} \\ &\quad\cdot\int_{-\infty}^{\infty}\int_{-\infty}^{\infty}\frac{1}{1+e^{-w}}\,e^{-\frac{1}{4s^2(1-r^2)}\left((w-2m)^2(1-r)+z^2(1+r)\right)}\,dw\,dz, \end{aligned}$$

where the term $\frac{1}{2}$ is the Jacobian of the variable changes $\theta_i = \frac{w+z}{2}$ and $\theta_j = \frac{w-z}{2}$.

Finally, we observe that the double integral can be written as the product of two integrals, one of whom is the normal-logistic integral. Therefore, the expected density of the network can be expressed as

$$\begin{aligned}&\frac{1}{2}\frac{1}{2s^2\pi\sqrt{1-r^2}} \\ &\quad\cdot\int_{-\infty}^{\infty}\int_{-\infty}^{\infty}\frac{1}{1+e^{-w}}\,e^{-\frac{1}{4s^2(1-r^2)}\left((w-2m)^2(1-r)+z^2(1+r)\right)}\,dw\,dz \\ &\quad= \frac{1}{2}\frac{1}{2s^2\pi\sqrt{1-r^2}}\int_{-\infty}^{\infty}e^{-\frac{z^2(1+r)}{4s^2(1-r^2)}}\,dz \\ &\qquad\cdot\int_{-\infty}^{\infty}\frac{1}{1+e^{-w}}\,e^{-\frac{(w-2m)^2(1-r)}{4s^2(1-r^2)}}\,dw \\ &\quad= \frac{1}{2}\frac{\sqrt{2}\sqrt{\pi}s\sqrt{1-r}}{2\sigma^2\pi\sqrt{1-r^2}}\int_{-\infty}^{\infty}\frac{1}{1+e^{-w}}\,e^{-\frac{(w-2m)^2}{4s^2(1+r)}}\,dw \\ &\quad= \frac{1}{2}\frac{\sqrt{1-r}}{s\sqrt{2}\sqrt{\pi}\sqrt{1-r^2}}\int_{-\infty}^{\infty}\frac{1}{1+e^{-w}}\,e^{-\frac{(w-2m)^2}{4\sigma^2(1+r)}}\,dw \\ &\quad= I\left(2m, 2s^2(1+r)\right). \end{aligned}$$

APPENDIX B: PROOF OF PROPOSITION 1

In this appendix, we prove Proposition 1 in Sec. III. Let f be a network metric and indicating with $\{\vec{\theta}\}_{0:\tau}$ the past history of the fitness vector, it is possible to write explicitly the expected value of the network metric f conditioned to the history of $\vec{\theta}_t$ from 0 to time τ as

$$\mathbb{E}[f(\mathbf{A}_t)|\{\vec{\theta}\}_{0:\tau}] = \int \mathbb{E}\left[f(\mathbf{A}_t)|\vec{\theta}_t\right] P\left(\vec{\theta}_t|\{\vec{\theta}\}_{0:\tau}\right) d\vec{\theta}_t. \tag{B1}$$

Given the Markovianity and Gaussianity of our setting, Eq. (B1) becomes

$$\begin{aligned}\mathbb{E}[f(\mathbf{A}_t)|\{\vec{\theta}\}_{0:\tau}] &= \int \mathbb{E}\left[f(\mathbf{A}_t)|\vec{\theta}_t\right] P\left(\vec{\theta}_t|\vec{\theta}_\tau\right) d\vec{\theta}_t \\ &= \int \mathbb{E}\left[f(\mathbf{A}_t)|\vec{\theta}_t\right] \mathcal{N}\left(\vec{\theta}_t; \vec{\mu}_t, \mathbf{\Sigma}_t\right) d\vec{\theta}_t, \end{aligned} \tag{B2}$$

where $\vec{\mu}_t$ and $\mathbf{\Sigma}_t$ are, respectively, the conditional mean and variance of $\vec{\theta}_t|\{\vec{\theta}\}_{0:\tau}$ in Eqs. (19) and (20). By Eq. (17), the IRF for the network metric f is defined as

$$\begin{aligned}\mathit{IRF}^f(t; \vec{\Delta\theta}) = \mathbb{E}[f(\mathbf{A}_{t+\tau})|\vec{\theta}_\tau + \vec{\Delta\theta}, \vec{\theta}_{\tau-1}, \cdots] \\ - \mathbb{E}[f(\mathbf{A}_{t+\tau})|\vec{\theta}_\tau, \vec{\theta}_{\tau-1}, \cdots],\end{aligned}$$

and by using (B2), it is possible to write the IRF as a Gaussian integration as

$$\begin{aligned}\mathit{IRF}^f(t; \vec{\Delta\theta}) = \int \mathbb{E}\left[f(\mathbf{A}_t)|\vec{\theta}_t\right] \\ \cdot \left[\mathcal{N}\left(\vec{\theta}_t; \vec{\mu}_t + \mathbf{B}^{t-\tau}\vec{\Delta\theta}, \mathbf{\Sigma}_t\right) - \mathcal{N}\left(\vec{\theta}_t; \vec{\mu}_t, \mathbf{\Sigma}_t\right)\right] d\vec{\theta}_t.\end{aligned}$$

APPENDIX C: POWER OF VAR MATRIX IN MEAN-FIELD MODEL

As assumed in Sec. IV, we deal with a full matrix $\mathbf{B}$ whose diagonal elements are all equal to a and the off-diagonal elements are equal to b. Observing that such a matrix can be written as $\mathbf{B} = (a-b)\mathbf{I} + b\mathbf{1}$, where $\mathbf{I}$ is the identity matrix and $\mathbf{1}$ is the matrix whose elements are all one, then the t-power of such a matrix can be written as

$$\mathbf{B}^t = \mathbf{I}(a-b)^t + \frac{\lambda_1^t - (a-b)^t}{n}\mathbf{1}. \tag{C1}$$

We use Eq. (C1) to write analytically the conditional mean and the conditional variance in Eqs. (19) and (20), respectively. For simplicity, we assume that $\tau = 0$, and first, we explicitly write the following geometric sum:

$$\mathbf{I} + \mathbf{B}^1 + \mathbf{B}^2 + \cdots + \mathbf{B}^{t-1} = \sum_{k=0}^{t-1} \mathbf{B}^k,$$

which is equal to

$$\mathbf{I}\frac{1-(a-b)^t}{1-(a-b)} + \mathbf{1}\left[\frac{1-\lambda_1^t}{1-\lambda_1} - \frac{1-(a-b)^t}{1-(a-b)}\right]\frac{1}{n}.$$

By the same reasoning, it is possible to derive the power function as

$$\begin{aligned}&\mathbf{I} + \mathbf{B}^2 + \mathbf{B}^4 + \cdots + \mathbf{B}^{2(t-1)} \\ &= \sum_{k=0}^{t-1} \mathbf{B}^{2k} = \mathbf{I}\frac{1-(a-b)^{2t}}{1-(a-b)^2} + \mathbf{1}\left[\frac{1-\lambda_1^{2t}}{1-\lambda_1^2} - \frac{1-(a-b)^{2t}}{1-(a-b)^2}\right]\frac{1}{n}.\end{aligned}$$

REFERENCES

Ackermann, J., "The subprime crisis and its consequences," J. Financ. Stab. **4**, 329–337 (2008).

Albert, R., Jeong, H., and Barabási, A.-L., "Error and attack tolerance of complex networks," Nature **406**, 378–382 (2000).

Allen, F. and Carletti, E., "An overview of the crisis: Causes, consequences, and solutions," Int. Rev. Finance **10**, 1–26 (2010).

Artime, O., Grassia, M., De Domenico, M., Gleeson, J. P., Makse, H. A., Mangioni, G., Perc, M., and Radicchi, F., "Robustness and resilience of complex networks," Nat. Rev. Phys. **6**, 114–131 (2024).

Bardoscia, M., Barucca, P., Battiston, S., Caccioli, F., Cimini, G., Garlaschelli, D., Saracco, F., Squartini, T., and Caldarelli, G., "The physics of financial networks," Nat. Rev. Phys. **3**, 490–507 (2021).

Barucca, P. and Lillo, F., "Disentangling bipartite and core-periphery structure in financial networks," Chaos Soliton. Fract. **88**, 244–253 (2016).

Barucca, P. and Lillo, F., "The organization of the interbank network and how ECB unconventional measures affected the e-MID overnight market," Comput. Manage. Sci. **15**, 33–53 (2018).

Battiston, S., Farmer, J. D., Flache, A., Garlaschelli, D., Haldane, A. G., Heesterbeek, H., Hommes, C., Jaeger, C., May, R., and Scheffer, M., "Complexity theory and financial regulation," Science **351**, 818–819 (2016).

Bianconi, G. and Barabási, A.-L., "Competition and multiscaling in evolving networks," Europhys. Lett. **54**, 436 (2001).

Boccaletti, S., Latora, V., Moreno, Y., Chavez, M., and Hwang, D.-U., "Complex networks: Structure and dynamics," Phys. Rep. **424**, 175–308 (2006).

Buccheri, G. and Mazzarisi, P., "Realized random graphs, with an application to the interbank network," J. Financ. Econom. **2024**, nbae024.

Burger, M., Van Oort, F., and Linders, G.-J., "On the specification of the gravity model of trade: Zeros, excess zeros and zero-inflated estimation," Spatial Econ. Anal. **4**, 167–190 (2009).

Caccioli, F., Barucca, P., and Kobayashi, T., "Network models of financial systemic risk: A review," J. Comput. Social Sci. **1**, 81–114 (2018).

Caldarelli, G., Capocci, A., De Los Rios, P., and Munoz, M. A., "Scale-free networks from varying vertex intrinsic fitness," Phys. Rev. Lett. **89**, 258702 (2002).

Campajola, C., Gangi, D. D., Lillo, F., and Tantari, D., "Modelling time-varying interactions in complex systems: The score driven kinetic Ising model," Sci. Rep. **12**, 19339 (2022).

Cerqueti, R., Cinelli, M., Ferraro, G., and Iovanella, A., "Financial interbanking networks resilience under shocks propagation," Ann. Oper. Res. **330**, 389–409 (2023).

Chatterjee, S., Diaconis, P., and Sly, A., "Random graphs with a given degree sequence," Ann. Appl. Probab. **21**(4), 1400–1435 (2011).

Cimini, G., Squartini, T., Garlaschelli, D., and Gabrielli, A., "Systemic risk analysis on reconstructed economic and financial networks," Sci. Rep. **5**, 15758 (2015).

Demidenko, E., *Mixed Models: Theory and Applications with R* (John Wiley & Sons, 2013).

Di Gangi, D., Bormetti, G., and Lillo, F., "Score-driven generalized fitness model for sparse and weighted temporal networks," Inf. Sci. **612**, 1226–1245 (2022).

Easley, D., Kleinberg, J. *et al.*, *Networks, Crowds, and Markets: Reasoning About a Highly Connected World* (Cambridge University Press, Cambridge, 2010), Vol. 1.

Eisenberg, L. and Noe, T. H., "Systemic risk in financial systems," Manage. Sci. **47**, 236–249 (2001).

Erdos, P. and Renyi, A., "On random graph," Publ. Math. **6**, 290–297 (1959).

Estrada, E., *The Structure of Complex Networks: Theory and Applications* (American Chemical Society, 2012).

Ferraro, G. and Iovanella, A., "Clairvoyant targeted attack on complex networks," Int. J. Comput. Econ. Econom. **8**, 41–62 (2018).
Freixas, X. and Rochet, J.-C., *Microeconomics of Banking* (MIT Press, 2008).
Fricke, D. and Lux, T., "Core–periphery structure in the overnight money market: Evidence from the e-MID trading platform," Comput. Econ. **45**, 359–395 (2015).
Fricke, D. and Lux, T., "On the distribution of links in the interbank network: Evidence from the e-MID overnight money market," Empirical Econ. **49**, 1463–1495 (2015).
Gabrielli, A., Mastrandrea, R., Caldarelli, G., and Cimini, G., "Grand canonical ensemble of weighted networks," Phys. Rev. E **99**, 030301 (2019).
Gao, J., Barzel, B., and Barabási, A.-L., "Universal resilience patterns in complex networks," Nature **530**, 307–312 (2016).
Giraitis, L., Kapetanios, G., Wetherilt, A., and Žikeš, F., "Estimating the dynamics and persistence of financial networks, with an application to the sterling money market," J. Appl. Econ. **31**, 58–84 (2016).
Glasserman, P. and Young, H. P., "Contagion in financial networks," J. Econ. Lit. **54**, 779–831 (2016).
Glasserman, P. and Young, H. P., "How likely is contagion in financial networks? J. Banking Finance **50**, 383–399 (2015).
Harris, J. K., *An Introduction to Exponential Random Graph Modeling* (Sage Publications, 2013), Vol. 173.
Holland, P. W. and Leinhardt, S., "An exponential family of probability distributions for directed graphs," J. Am. Stat. Assoc. **76**, 33–50 (1981).
Holme, P. and Saramäki, J., "Temporal networks," Phys. Rep. **519**, 97–125 (2012).
Iori, G., De Masi, G., Precup, O. V., Gabbi, G., and Caldarelli, G., "A network analysis of the Italian overnight money market," J. Econ. Dyn. Control **32**, 259–278 (2008).
Iori, G., Jafarey, S., and Padilla, F. G., "Systemic risk on the interbank market," J. Econ. Behav. Organ. **61**, 525–542 (2006).
Iori, G., Kapar, B., and Olmo, J., "Bank characteristics and the interbank money market: A distributional approach," Stud. Nonlinear Dyn. Econom. **19**, 249–283 (2015).
Iori, G., Mantegna, R. N., Marotta, L., Micciche, S., Porter, J., and Tumminello, M., "Networked relationships in the e-MID interbank market: A trading model with memory," J. Econ. Dyn. Control **50**, 98–116 (2015).
Katz, L., "A new status index derived from sociometric analysis," Psychometrika **18**, 39–43 (1953).
Khodarahmi, M. and Maihami, V., "A review on Kalman filter models," Arch. Comput. Methods Eng. **30**, 727–747 (2023).
Kobayashi, T. and Takaguchi, T., "Identifying relationship lending in the interbank market: A network approach," J. Banking Finance **97**, 20–36 (2018).
Lütkepohl, H., *New Introduction to Multiple Time Series Analysis* (Springer Science & Business Media, 2005).
Lütkepohl, H., *Impulse Response Function* (Springer, 2010).
Lusher, D., Koskinen, J., and Robins, G., *Exponential Random Graph Models for Social Networks: Theory, Methods, and Applications* (Cambridge University Press, 2013).
Mata, A. S. D., "Complex networks: A mini-review," Braz. J. Phys. **50**, 658–672 (2020).
May, R. M., Levin, S. A., and Sugihara, G., "Ecology for bankers," Nature **451**, 893–894 (2008).
Mazzarisi, P., Barucca, P., Lillo, F., and Tantari, D., "A dynamic network model with persistent links and node-specific latent variables, with an application to the interbank market," Eur. J. Oper. Res. **281**, 50–65 (2020).
Mazzarisi, P. and Lillo, F., "Methods for reconstructing interbank networks from limited information: A comparison," in *Econophysics and Sociophysics: Recent Progress and Future Directions* (Springer, 2017), pp. 201–215.
Sanders, A., "The subprime crisis and its role in the financial crisis," J. Hous. Econ. **17**, 254–261 (2008).
Temizsoy, A., Iori, G., and Montes-Rojas, G., "Network centrality and funding rates in the e-MID interbank market," J. Financ. Stab. **33**, 346–365 (2017).
Winkelmann, R., *Econometric Analysis of Count Data* (Springer Science & Business Media, 2008).
Yan, T., Jiang, B., Fienberg, S. E., and Leng, C., "Statistical inference in a directed network model with covariates," J. Am. Stat. Assoc. **114**, 857–868 (2019).